AD-A089 145 GENERAL ELECTRIC CORPORATE RESEARCH AND DEVELOPMENT --ETC F/G 11/6
ORIGIN OF MAGNETIC PROPERTIES IN AMORPHOUS METALS.(U)
DEC 79 F E LUBORSKY, J J BECKER N00014-76-C-0807
UNCLASSIFIED SRD-80-006 NL

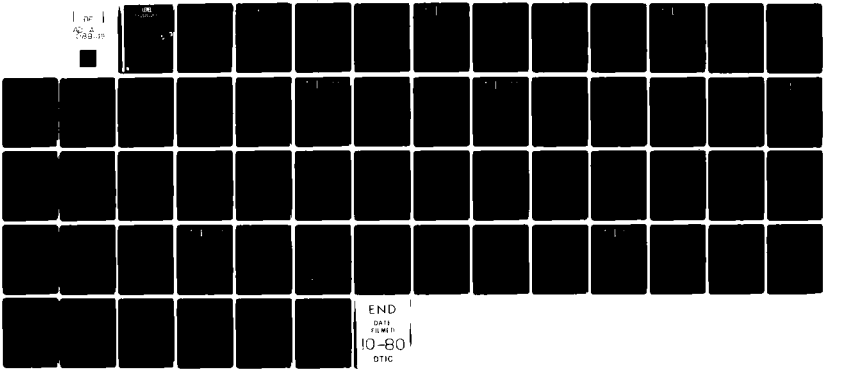

END
DATE FILMED
10-80
DTIC

LEVEL II

12

ORIGIN OF MAGNETIC PROPERTIES IN AMORPHOUS METALS

Interim Report
to the
Office of Naval Research
Contract N00014-76-C-0807

Submitted by
F.E. Luborsky and J.J. Becker

January 1980

General Electric Company
Corporate Research and Development
Schenectady, NY 12301

SRD-80-006

UNCLASSIFIED

SECURITY CLASSIFICATION OF THIS PAGE (When Data Entered)

REPORT DOCUMENTATION PAGE	READ INSTRUCTIONS BEFORE COMPLETING FORM
1. REPORT NUMBER	2. GOVT ACCESSION NO. AD-A089 145 (9) 3. RECIPIENT'S CATALOG NUMBER Summary Technical Report, 1 Oct 78-1 Dec 7
4. TITLE (and Subtitle) (6) Summary Technical Report on the Origin of Magnetic Properties in Amorphous Metals, October 1, 1978 to December 1, 1979	5. TYPE OF REPORT & PERIOD COVERED ONR Technical Report
	6. PERFORMING ORG. REPORT NUMBER (14) SRD-80-006
7. AUTHOR(s) (10) F. E. Luborsky and J. J. Becker	8. CONTRACT OR GRANT NUMBER(s) N00014-76-0807 (15) N00014-76-C-0807
9. PERFORMING ORGANIZATION NAME AND ADDRESS General Electric Co. Corporate Research & Development Center Schenectady, NY 12301	10. PROGRAM ELEMENT, PROJECT, TASK AREA & WORK UNIT NUMBERS
11. CONTROLLING OFFICE NAME AND ADDRESS Office of Naval Research Metallurgy Program Arlington, VA 22217	12. REPORT DATE (11) December 1979 13. NUMBER OF PAGES (12) 60
14. MONITORING AGENCY NAME & ADDRESS (if different from Controlling Office)	15. SECURITY CLASS. (of this report) Unclassified
	15a. DECLASSIFICATION/DOWNGRADING SCHEDULE

16. DISTRIBUTION STATEMENT (of this Report)

Approved for public release; distribution unlimited.

17. DISTRIBUTION STATEMENT (of the abstract entered in Block 20, if different from Report)

18. SUPPLEMENTARY NOTES

19. KEY WORDS (Continue on reverse side if necessary and identify by block number)

Amorphous Metals, Magnetic Properties, Crystallization, Magnetic Ordering, Stress Relief, Stress Relaxation

20. ABSTRACT (Continue on reverse side if necessary and identify by block number)

The magnetic properties of amorphous metals are examined relative to changes in composition and heat treatment of amorphous transition metal-metalloid alloys. The transition metals examined were iron and iron plus nickel. These were alloyed with the metalloids boron, silicon and carbon. Significant effects of alloy variation were observed on magnetic properties and on the crystallization and stress relief of these materials. The effects of stress on magnetic properties was studied.

DD FORM 1 JAN 73 1473 EDITION OF 1 NOV 65 IS OBSOLETE S/N 0102-LF-014-6601

UNCLASSIFIED

SECURITY CLASSIFICATION OF THIS PAGE (When Data Entered)

406611

GENERAL ELECTRIC

CORPORATE RESEARCH AND DEVELOPMENT

GENERAL ELECTRIC COMPANY, RESEARCH AND DEVELOPMENT CENTER, P.O. BOX 8
SCHENECTADY, NEW YORK 12301, Phone (518) 385-2211

December 12, 1979

Arthur M. Diness, Director
Metallurgy and Ceramics Program
Office of Naval Research
Arlington, VA 22217

Subject: ONR Contract N00014-76-C-0807
"Investigation into the Origin of Magnetic Properties of Amorphous Metallic Alloys"
End-of-Year Letter Report

The magnetic properties of amorphous iron based alloys continue to exhibit characteristics which are extremely desirable for low loss magnetic devices and in particular for distribution transformers. Work has been continuing to explore the fundamental characteristics of amorphous alloys with the ultimate applied goal of applying them in distribution transformers. In this technical report we include reprints and preprints on various aspects of our alloy development aimed at finding alloys with increased saturation magnetization; on modeling the magnetic anisotropy to explain the induced anisotropy; on the effect of nickel on the magnetic properties; on stress relaxation effects which have implications for interpreting the structure of amorphous alloys; and on various aspects of the effects of stress on properties.

The effects of stress on the magnetic properties has been shown to be due to first, of course, the direct interaction of the stress with the magnetostriction but secondly it is also due to the development, on annealing, of a stress induced anisotropy. This stress induced anisotropy has a major influence on the properties of wound toroids but there have been no systematic studies published so far. We thus plan in the coming year to begin a study of stress induced anisotropy in amorphous alloys.

A summary of our most significant results is as follows:

1. We found a ridge of constant saturation magnetization in the Fe-B-Si ternary alloys extending from $Fe_{80}B_{20}$ to $Fe_{82}B_{13}Si_5$. Silicon additions increased the ease of formation and stability and lowered the losses without lowering saturation magnetization.

2. In the Fe-B-C ternary alloys a wider ridge of constant magnetization was found which extended out to $Fe_{83}B_{10}C_7$. However, the stability is decreased and losses increased.

3. The losses of alloys in the series $(Fe_xNi_{1-x})_{80}B_{20}$ exhibited a peak at x = 75% corresponding to the peak in the induced anisotropy. Permeabilities exhibited a minimum at the same composition.

4. The stress relaxation of Fe_xB_{100-x} alloys increased approximately linearly with x and with thickness. There was no evidence for any discontinuity in stress relaxation versus x as previously found for activation energy for crystallization. Thus different atomic processes are involved.

5. The magnetization versus temperature for various amorphous alloys was used to determine the spin wave stiffness constant, D. Linear D versus Curie temperature relations were observed which extrapolated to zero D at finite T_c. This behavior was qualitatively interpreted on the basis of the itinerant electron model.

6. The magnetic properties of toroids were found to improve with increase in toroid diameter even after stress relaxation anneals. This was attributed to a strain induced ordering anisotropy.

7. Crystallized amorphous iron alloys were shown to have potential as low cost permanent magnet materials. A $Fe_{40}Ni_{40}P_{20}$ alloy given a crystallization treatment of 15 minutes at 525 C developed a coercive force of 365 Oe, and saturation magnetization of about 8900 G. Other alloys have developed properties that would be excellent for hysteresis motor applications, especially since the alloys contain no cobalt or other strategic materials.

BIBLIOGRAPHY

The following papers are included in this technical report:

1. "Engineering Magnetic Properties of Fe-Ni-B Amorphous Alloys," F. E. Luborsky, J. L. Walter, and H. H. Liebermann, IEEE Trans. on Magnetics MAG-15, 909 (1979). Also GE Report 78CRD132.

2. "Formation and Magnetic Properties of Fe-B-Si Amorphous Alloys," F. E. Luborsky, J. J. Becker, J. L. Walter, and H. H. Liebermann, IEEE Trans. on Magnetics MAG-15, 1146 (1979). Also GE Report 79CRD053.

GENERAL ELECTRIC

BIBLIOGRAPHY, Continued

3. "Stress Relaxation of Iron-Boron Amorphous Alloys,"

   F. E. Luborsky and H. H. Liebermann, J. Appl. Phys., to appear. Also GE Report 79CRD177.

4. "The Effect of Temperature on Magnetic Saturation of Some Amorphous Alloys,"

   F. E. Luborsky, E. P. Wohlfarth, J. L. Walter and H. H. Liebermann, Magnetism and Magnetic Materials, to appear. Also GE Report 79CRD178.

5. "Strain Induced Anisotropy in Amorphous Alloys and the Effect of Toroid Diameter on Magnetic Properties,"

   F. E. Luborsky and J. J. Becker, IEEE Trans. Magnetics, to appear. Also GE Report 79CRD134.

6. "The Fe-B-C Ternary Amorphous Alloys,"

   F. E. Luborsky, J. J. Becker, J. L. Walter, and D. L. Martin, IEEE Trans. Magnetics, to appear. Also GE Report 79CRD169.

7. "Amorphous Materials - A New Class of Soft Magnetic Alloys,"

   F. E. Luborsky, P. G. Frischmann, and L. A. Johnson, J. Magnetism Magn. Mat., accepted. Also GE Report 79CRD209.

R. G. Rowe, Manager
Properties Branch
METALLURGY LABORATORY

GENERAL ELECTRIC

General Electric Company
Corporate Research and Development
Schenectady, New York

TECHNICAL INFORMATION SERIES

AUTHOR	SUBJECT	NO
Luborsky, FE Walter, JL Liebermann, HH	amorphous magnetic alloys	78CRD132
		DATE: July 1978
TITLE: Engineering Magnetic Properties of Fe-Ni-B Amorphous Alloys		GE CLASS: 1
		NO PAGES: 3
ORIGINATING COMPONENT: Metallurgy Laboratory		CORPORATE RESEARCH AND DEVELOPMENT SCHENECTADY, N.Y.

SUMMARY

Amorphous alloys in the series $(Fe_xNi_{1-x})_{80}B_{20}$ with $20 < x < 80$ were prepared by melt spinning. Losses and permeabilities are reported for frequencies from 100 Hz to 100 kHz. The as-wound toroids showed an increase in losses and a decrease in permeability with increasing x, consistent with the increase in magnetostriction observed with increasing x. After stress relief annealing of the toroids, maximum losses were observed at x = 75. This composition corresponds to the composition at which the magnetic anneal anisotropy is maximum.

KEY WORDS

magnetic alloys, transformer alloys, amorphous alloys

INFORMATION PREPARED FOR _____

Additional Hard Copies Available From

Corporate Research & Development Distribution
P.O. Box 43 Bldg. 5, Schenectady, N.Y., 12301

Microfiche Copies Available From

Technical Information Exchange
P.O. Box 43 Bldg. 5, Schenectady, N.Y., 12301

ENGINEERING MAGNETIC PROPERTIES OF Fe-Ni-B AMORPHOUS ALLOYS

F.E. Luborsky, J.L. Walter, and H.H. Liebermann

The technical properties of a variety of amorphous alloy compositions have been reported in previous papers. (Refs. 1-3) It appeared that the magnetic losses and permeabilities improved as the magnetostriction of the alloys decreased, but there was considerable scatter in the results presumably because alloys of the different compositions, i.e., $(Fe, Ni)_{80}B_{20}$, $(Fe, Ni)_{80}P_{14}B_6$, and $Fe_3Co_{72}P_{16}B_6Al_3$, were compared.

This report will discuss the technical properties of the series $(Fe_xNi_{1-x})_{80}B_{20}$ amorphous alloys. Fundamental magnetic properties such as moments, Curie temperatures[4,5] and induced anisotropy[6-9] have already been reported along with crystallization.[10] The magnetostriction decreases from 31×10^{-6} for $Fe_{80}B_{20}$ to $\sim 3 \times 10^{-6}$ for $(Fe_{.25}Ni_{.75})_{80}B_{20}$.[11,12]

Amorphous alloy ribbons were prepared by directing a molten stream of metal onto the surface of a rotating drum.[13] About 10 to 15 turns of ribbon were then wound into an open aluminum or tungsten core box with an average diameter of 1.4 cm. Fifty turns of wire insulated with high temperature enamel were wound on the box for drive and for sense windings. DC hysteresis loops were obtained using an integrating flux meter. ac losses and permeabilities were obtained from 100 Hz to 100 kHz as a function of drive field using a sine H drive. To measure losses, a volt-ampere-phase shift measurement was used where the total losses are

$$W = VI\cos\theta/v \qquad (1)$$

where V = rms signal voltage, I = rms drive current, v = sample volume, and θ = phase shift. The permeabilities were calculated using

$$\mu_z = V\ell 10^8/8fIN^2A \qquad (2)$$

where ℓ = magnetic path length, f = frequency, N = turns of wire on the core, and A = cross section of magnetic material. The maximum inductions were calculated using

$$B_m = V10^8/4.44\ fNA \qquad (3)$$

and the peak drive field

$$H = 0.4\pi NI/C$$

where C is the circumference of the wire winding on the coil.

The results of the dc measurements are shown in Figs. 1 to 3. In Fig. 1 the saturation magnetizations, $4\pi M_s$, at room temperature confirm previous reports[4,5] and extend them to lower iron contents. The coercivities, H_c, and remanence to saturation ratio, M_r/M_s, are shown in Figs. 2 and 3. In the as-wound toroids both H_c and M_r/M_s are essentially independent of composition but show a slight rise with increasing iron content. This slight rise is expected if we assume that the samples were prepared under the same conditions so that the quenched-in residual stresses and the stresses incurred in winding the toroid are all the same as a function of iron. The stresses interact with the increasing magnetostriction, λ, resulting from the increased iron content. This enhanced magnetoelastic response

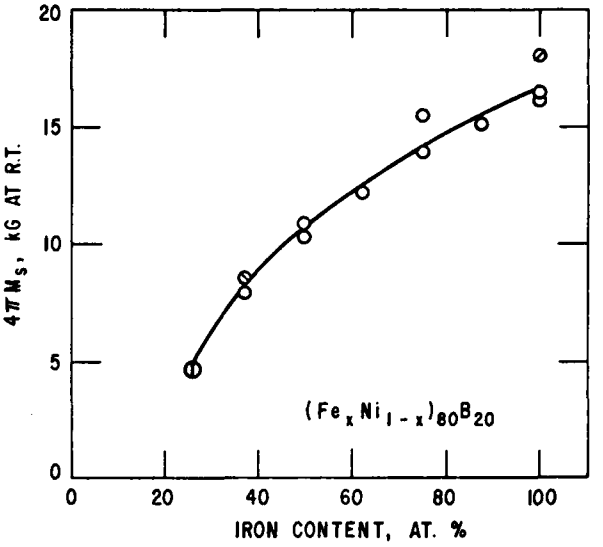

Fig. 1 Room temperature saturation magnetization as a function of iron content in Fe-Ni-B amorphous alloys. ⊕(Fe, Ni)$_{80}B_{19}P_1$, ⊘(Fe, Ni)$_{80}B_{10}Si_{10}$, ⊘$Fe_{82}B_{18}$.

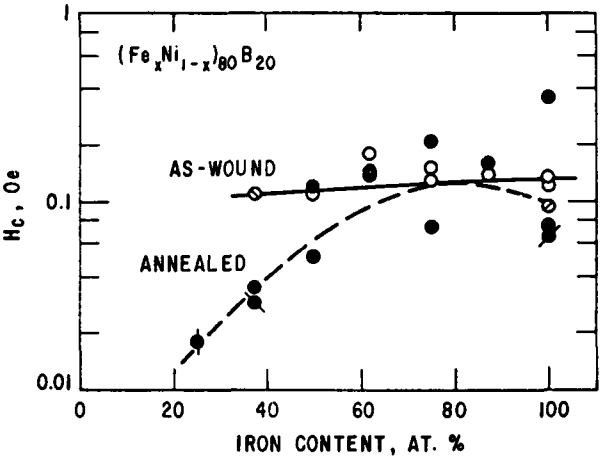

Fig. 2 Coercive field of as-wound and annealed amorphous alloy toroids. Samples annealed to minimum H_c in circumferential H. Same symbols as in Fig. 1.

results in an increase in anisotropy, K_λ, which is directly responsible for the increase in H_c. After toroidally winding, the samples were then annealed at 25°C intervals, in a circumferential field, starting at 275°C to approximately 375°C. The minimum H_c achieved by these anneals are shown in Fig. 2 by the dashed line. Note the peak in this curve at ~75% iron. A similar peak appears in the M_r/M_s curve after annealing, shown in Fig. 3. We presume that this peak is the result of the peak in the magnetically-induced anisotropy as a function of x.[6] Core losses at 1 kG for sine H drive

Manuscript received May 24, 1978.

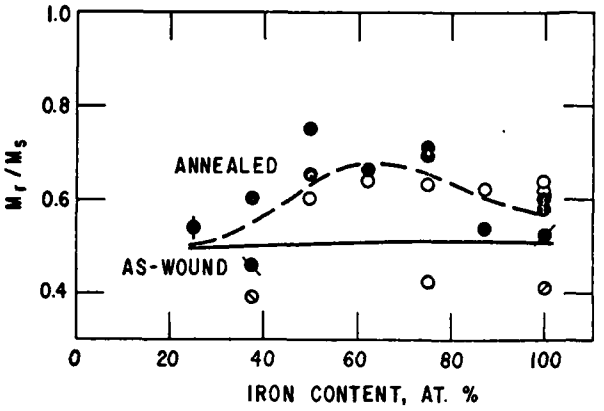

Fig. 3 Remanence to saturation ratio of as-wound and annealed amorphous alloy toroids. Samples annealed to minimum H_c in circumferential H. Same symbols as in Fig. 1.

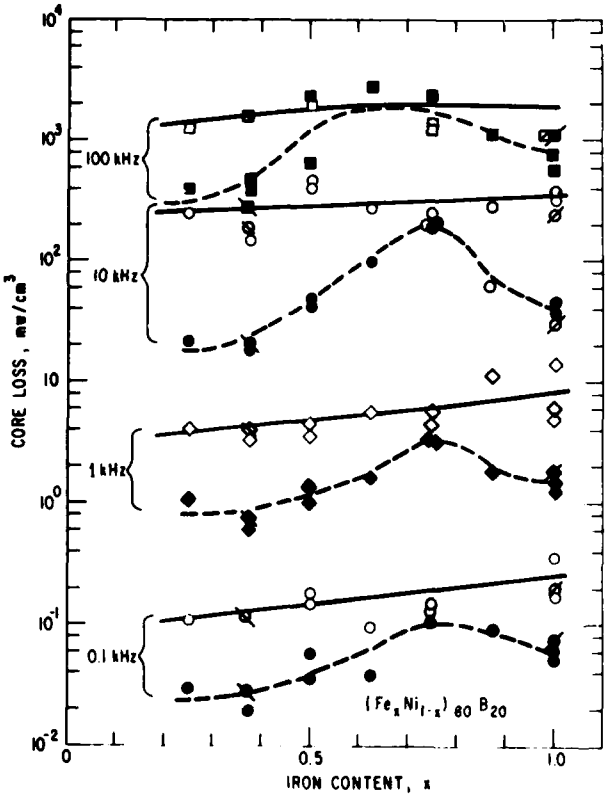

Fig. 4 Losses at various frequencies for as-wound—(and annealed)---amorphous alloy toroids. Sine H test at B_m = 1kG samples annealed to minimum H_c values. Same symbols as in Fig. 1

(Fig. 4) and permeability (Fig. 5) are shown as a function of frequency. The core losses of the as-wound ribbons increase with x and the permeabilities decrease with x. However, after annealing the losses show a peak at about 75% iron, and the permeability shows a minimum at the same value. Core losses at 3 kG show exactly the same trends as at 1 kG with $W \alpha f^{1.4\pm0.1}B_m^{1.8\pm0.2}$ for the annealed samples. The effect of measurement

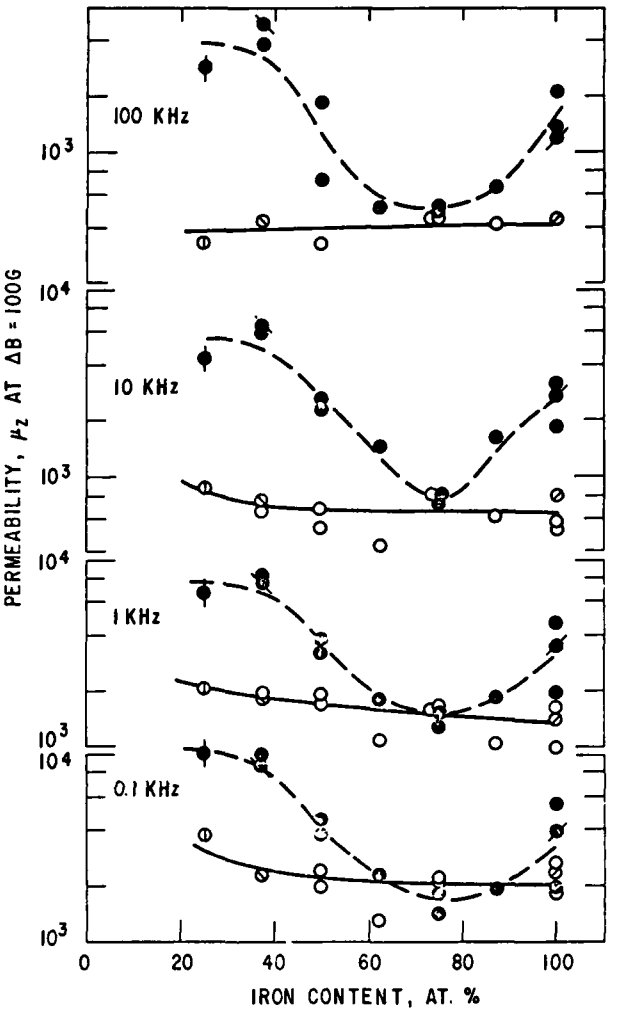

Fig. 5 "Initial" impedance permeability for as-wound —and annealed---amorphous alloy toroids. Samples annealed to minimum H_c values. Same symbols as in Fig. 1.

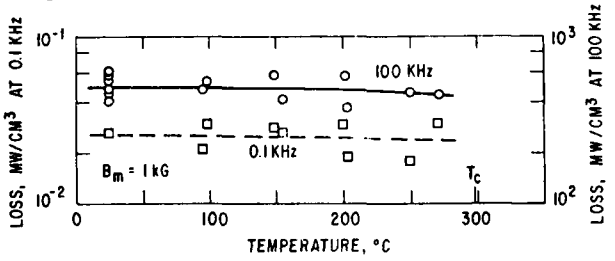

Fig. 6 Loss as a function of measurement temperature for toroids of amorphous $Fe_{30}Ni_{50}B_{20}$ at 0.1 kHz and at 100 kHz.

temperature on losses is negligible nearly up to T_c, as shown in Fig. 6. We presume that the peak in losses and the minimum in permeability at about 75 atomic % iron are the result of the maximum in the induced anisotropy, K_u, which also occurs[6] at 70 to 75 atomic % iron.

REFERENCES

1. F.E. Luborsky, J.J. Becker, and R.O. McCary, IEEE Trans. Magnetics MAG-11, 1644 (1975).

2. F.E. Luborsky, R.O. McCary, and J.J. Becker, Proc. Second Intern. Conf. Rapidly Quenched Metals, ed. by N.J. Grant and B.C. Giessen, MIT Press, Cambridge, Mass., 1976, p. 467.

3. F.E. Luborsky, Amorphous Magnetism II, ed. by R.A. Levy and R. Hasegawa, Plenum Press, NY, 1977, p. 345.

4. J.J. Becker, F.E. Luborsky, J.L. Walter, IEEE Trans. Magnetics MAG-13, 988 (1977).

5. R.C. O'Handley, R. Hasegawa, R. Ray, and C.P. Chou, Appl. Phys. Lett. 29, 330 (1976).

6. F.E. Luborsky and J.L. Walter, IEEE Trans. Magnetics, MAG-13, 953 (1977).

7. F.E. Luborsky and J.L. Walter, Materials Sci. Eng. 28, 77 (1977).

8. F.E. Luborsky and J.L. Walter, IEEE Trans. Magnetics MAG-13, 1635 (1977).

9. F.E. Luborsky, AIP Conf. Proc. No. 29, 209 (1976).

10. F.E. Luborsky, Materials Sci. Eng. 28, 139 (1977).

11. O'Handley, Amorphous Magnetism II, ed. by R.A. Levy and R. Hasegawa, Plenum Press, NY, 1977, p. 379.

12. F.E. Luborsky, Ferromagnetic Materials, ed. by E.P. Wohlfarth, North Holland Publ. Co., Amsterdam, expected in 1979, Chapter XX.

13. H.H. Liebermann and C.D. Graham, Jr., IEEE Trans. Magnetics MAG-12 921 (1976).

GENERAL ELECTRIC

General Electric Company
Corporate Research and Development
Schenectady, New York

TECHNICAL INFORMATION SERIES

AUTHOR F.E. Luborsky J.J. Becker J.L. Walter H.H. Liebermann	SUBJECT amorphous alloys	NO. 79CRD053 DATE March 1979
TITLE Formation and Magnetic Properties of Fe-B-Si Amorphous Alloys		GE CLASS 1 NO. PAGES 7
ORIGINATING COMPONENT Metallurgy Laboratory		CORPORATE RESEARCH AND DEVELOPMENT SCHENECTADY, N.Y.

SUMMARY

The magnetic properties and crystallization temperatures of alloys in the ternary Fe-B-Si system are reported. With the replacement of boron by silicon the Curie temperature increases slightly. This results in a sharp ridge of relatively constant room temperature saturation magnetization extending from $Fe_{80}B_{20}$ to $Fe_{82}B_{12}Si_6$. The coercivity exhibits a broad minimum, both before and after stress relief annealing, in the region around $Fe_{81}B_{15}Si_4$ and extending at least to $Fe_{77}B_{13}Si_{10}$. The crystallization temperature rises with increasing silicon and decreasing iron and boron. The alloys with silicon are generally easier to prepare in the amorphous state than the binary Fe-B alloys. Thus, for the highest saturation magnetization alloy combined with ease of preparation, stability, and lowest losses, the alloys between $Fe_{81}B_{17}Si_2$ and $Fe_{82}B_{12}Si_6$ are preferred.

KEY WORDS

amorphous magnetism, magnetic properties

INFORMATION PREPARED FOR _____

Additional Hard Copies Available From

Corporate Research & Development Distribution
P.O. Box 43 Bldg. 5, Schenectady, N.Y., 12301

Microfiche Copies Available From

Technical Information Exchange
P.O. Box 43 Bldg. 5, Schenectady, N.Y., 12301

FORMATION AND MAGNETIC PROPERTIES OF Fe-B-Si AMORPHOUS ALLOYS

F.E. Luborsky, J.J. Becker, J.L. Walter, and H.H. Liebermann

INTRODUCTION

In the iron-boron binary amorphous alloy series, the highest magnetic moment at low temperatures occurs in systems with the highest iron content. Amorphous ribbons have been made by melt-spinning with iron contents as high as 86-88 a/o iron [1-3] and with saturation magnetizations at 77 K, σ_s (77 K) = 210 emu/g [1]. However, for these same alloys at room temperature σ_s (298 K) = 163 emu/g [1] compared with the lower iron-containing amorphous alloy $Fe_{80}B_{20}$ which has the maximum σ_s at room temperature σ_s (298 K) = 180 emu/g [1-4]. This decrease at room temperature for the higher iron-rich alloys results from the rapid drop in Curie temperature, T_c, with increase in iron content. Thus, one approach to increasing σ_s (298 K) is to increase T_c. To do this without a substantial cost increase, no cobalt or nickel additions may be used. This leaves the possibility of varying the metalloid and its composition.

This paper considers the effects of adding silicon to iron-boron amorphous alloys. It is shown that although the addition of silicon raises T_c, its presence does not result in higher moments because of its greater propensity for donating electrons to the 3d transition metal band. However, silicon facilitates the preparation of tape and produces more stable alloys with lower coercivity and without a significant loss in σ_s (298 K).

EXPERIMENTAL

Amorphous ribbons were prepared [5] by chill block melt-spinning. Curie temperatures were determined using a thermogravimetric recording balance having a furnace fitted with a permanent magnet, to produce a field of 225 Oe and a field gradient. Samples were heated at 20 °/min. Magnetizations were determined using a vibrating sample magnetometer in fields up to 20 kOe. Results reported were obtained by extrapolating to $H = \infty$ using a $1/H^2$ function. Coercive fields, H_c, were determined for 10 cm long ribbons using an integrating fluxmeter. Annealing occurred in a 30 Oe field and the samples were cooled in the same field.

RESULTS AND DISCUSSION

Figure 1 shows the range of compositions for which amorphous alloy ribbons may be fabricated in the ternary Fe-B-Si systems. The amorphous nature was ascertained primarily by the lack of brittleness in the as-cast ribbons with x-ray diffraction being used to confirm these conclusions on some of the samples. The differences in the curves taken from the various authors' results [6-9] represent differences in preparation conditions such as ribbon thickness, quenching surface, melt temperature, etc. The ease of making the alloys improved with increasing silicon additions to binary Fe-B alloys. By this we mean that ductile samples with uniform geometry can be obtained more often or in thicker ribbons. The resultant thermal stability was evaluated by noting the temperature at which the H_c started to increase after successive 2 hr anneals at rising temperatures, and the temperature at which magnetization began to increase from zero on increasing the temperature by 20 °C/min. This increase in magnetization is the result of development of Fe and Fe_3B crystals, both with high Curie temperatures [10]. As shown in Figures 2(a) and 2(b), these results indicate an increased stability as silicon replaced boron and as the iron content decreased.

Figure 3 shows the results of Curie temperature measurements. Narita et al [7, 11] reported the data for the alloys in the silicon-rich region and Masumoto [8, 9] reported some results for Fe_{80}-alloys from $-B_{20}$ to $-B_8$. The results of Narita et al and Masumoto tend to be about 10° higher than T_c measured in this work where the data overlap. Note that the replacement of boron by silicon at constant iron raises T_c slightly in the boron-rich region.

Figure 4 shows the saturation magnetizations at room temperature. These are about 5% lower than the values Hoselitz reported [6]. There is a ridge of maximum σ_s (298 K) which extends from $Fe_{80}B_{20}$ to $Fe_{82}B_{12}Si_6$ with a decrease of only 1% in σ_s. The corresponding ridge at 100 °C, shown in Figure 5, shifts towards lower iron contents for the binary Fe-B but does not appear to have moved from the $Fe_{82}B_{12}Si_6$ region.

Manuscript received February 9, 1979.

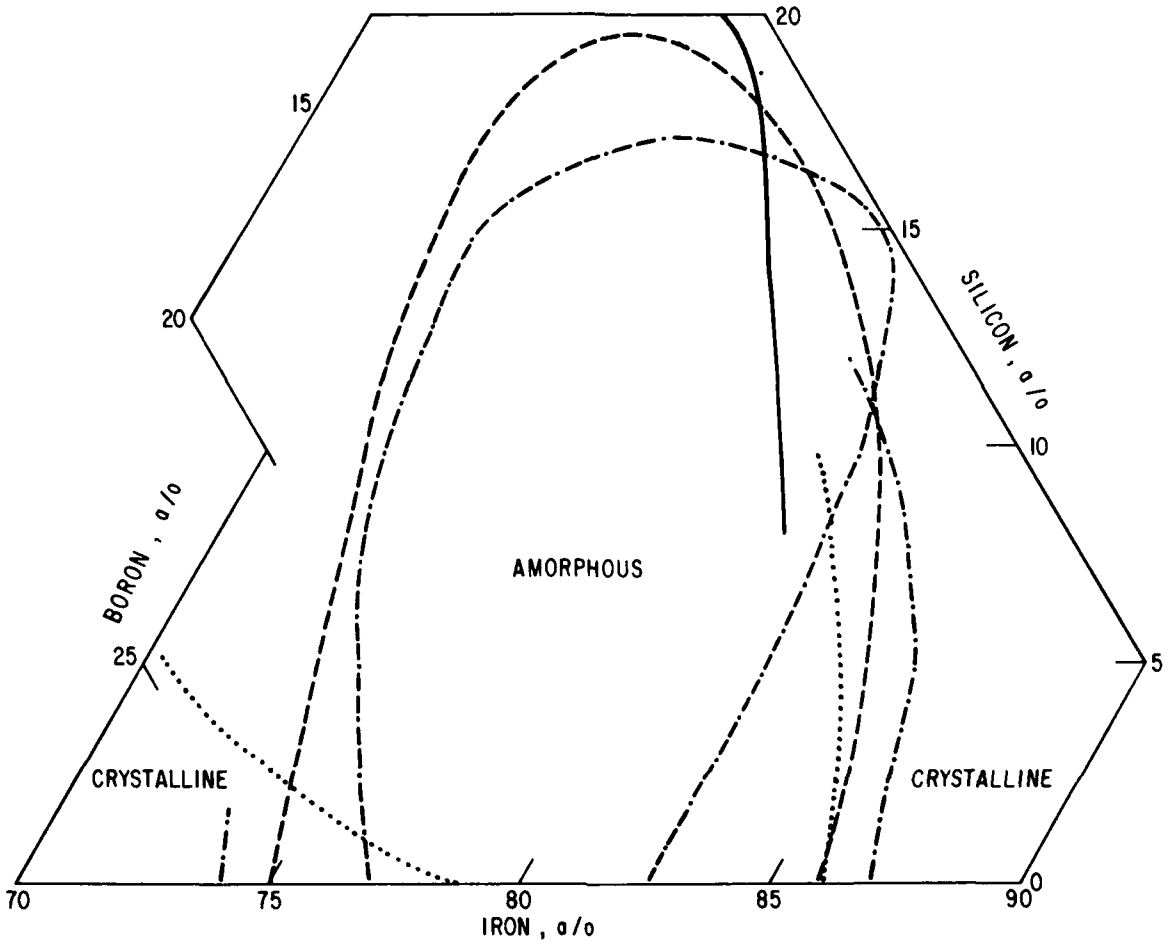

Figure 1. Preparation range for amorphous Fe-B-Si alloys. Reported by — — — — Masumoto, — —·— —·Inoue et al, ———— Narita et al, ····· Hoselitz, and —·—·—·—this work.

This ridge of maximum σ_s occurs for the same reason as discussed for the Fe-B amorphous alloys. That is, the rapid decrease in T_c, combined with an increase in iron, prevents the increase of σ_s with increase in iron. The small increase in T_c with replacement of B by Si does shift the peak σ_s to higher iron contents, as expected. However, the greater electron donor capacity of Si, as compared to B [12], decreases σ_s. This results in lower σ_s values at the same iron content; but since the peak σ_s occurs at higher iron contents, it fortuitously works out to produce the ridge of almost constant σ_s.

Figure 6 shows the coercive fields for as-cast samples, and Figure 7 shows coercivities after annealing to their minimum H_c. It is clear that a minimum H_c occurs with addition of 2 to 10% Si in the region of 77-82% Fe. It is presumed that this is the result of the decreasing magnetostriction with increase in silicon content. There are no results in the literature to confirm this assumption. This decrease in H_c results in a corresponding decrease in magnetic losses and an increase in permeability.

CONCLUSIONS

The highest saturation magnetization at room temperature in the Fe-B-Si system of amorphous alloys, occurs at $Fe_{80}B_{20}$. There is, however, a ridge of maximum room temperature σ_s which extends out to $Fe_{82}B_{12}Si_6$. The σ_s drops by about 1% from $Fe_{80}B_{20}$ to $Fe_{82}B_{12}Si_6$ while the coercivity decreases, and the ease of preparation and stability both improve with the addition of silicon. Thus, alloys containing silicon with about 80-82% Fe are the preferred alloys since they combine the highest σ_s with minimum H_c and losses, and improved ease of preparation and stability.

ACKNOWLEDGMENTS

We appreciate N. Marotta's work in obtaining the Curie temperatures and the magnetic measurements of Jim Gillespie. We are grateful to the Office of Naval Research for partial support of this work.

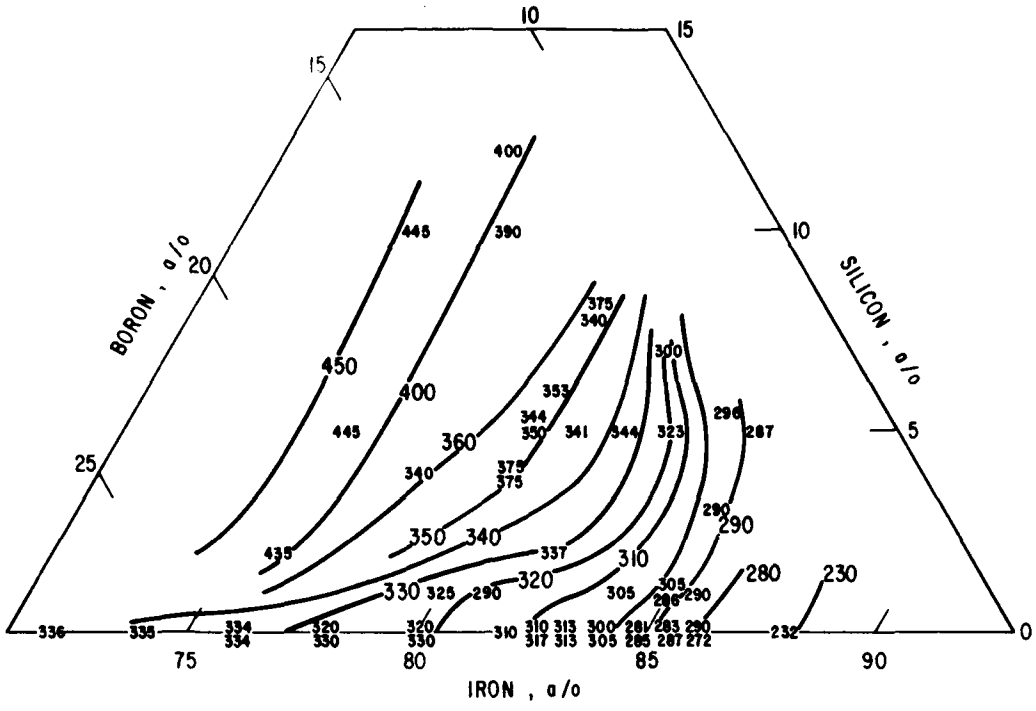

(a)

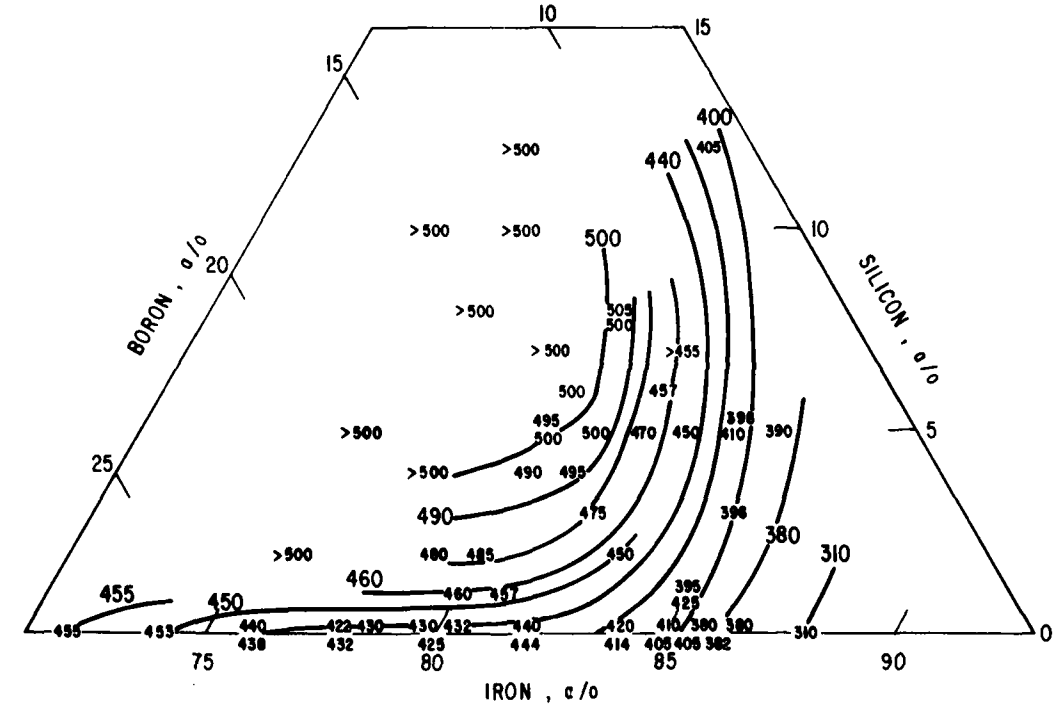

(b)

Figure 2. Temperature for start of crystallization (a) after 2 hour anneals, (b) after scanning temperatures at 20°C/min.

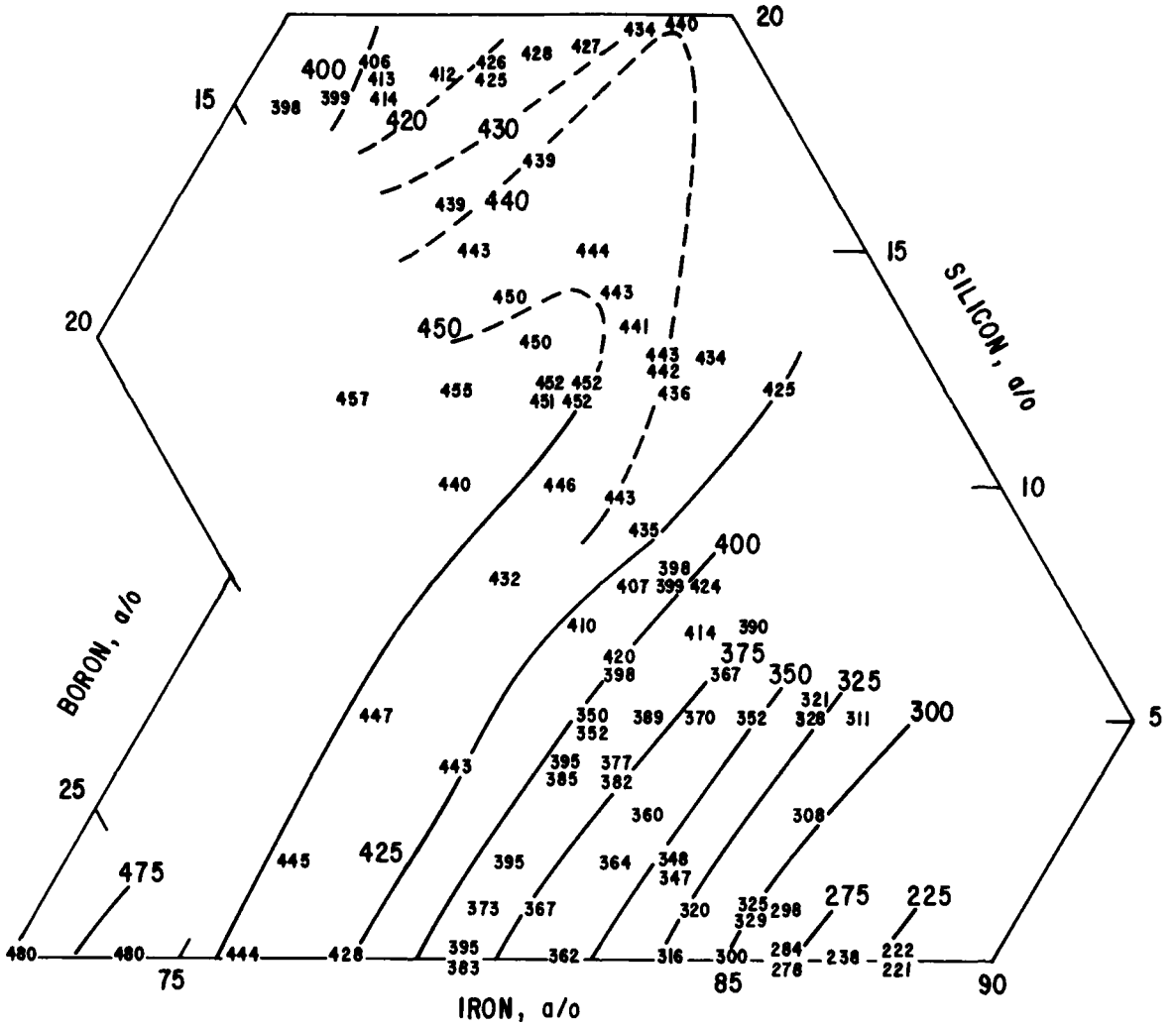

Figure 3. Curie temperatures of amorphous Fe-B-Si alloys. Solid lines from this work; dashed lines from Narita et al, °C.

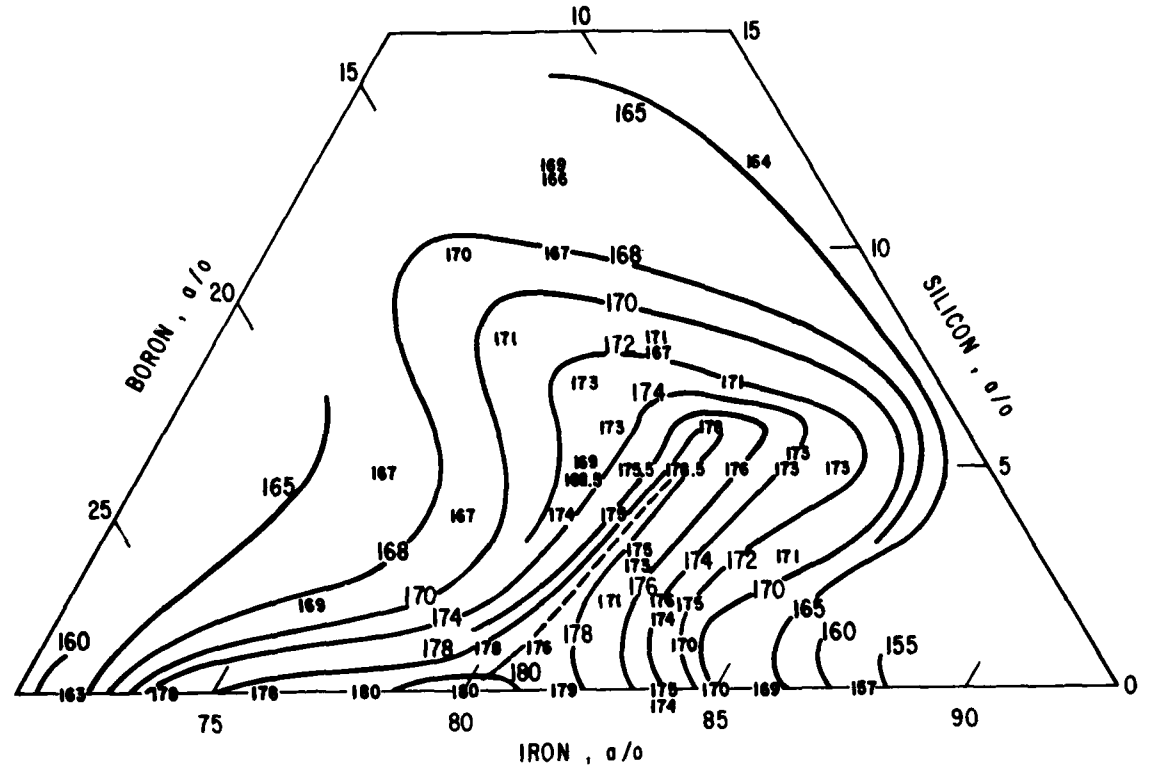

Figure 4. Saturation magnetization at room temperature for amorphous Fe-B-Si alloys, emu/g.

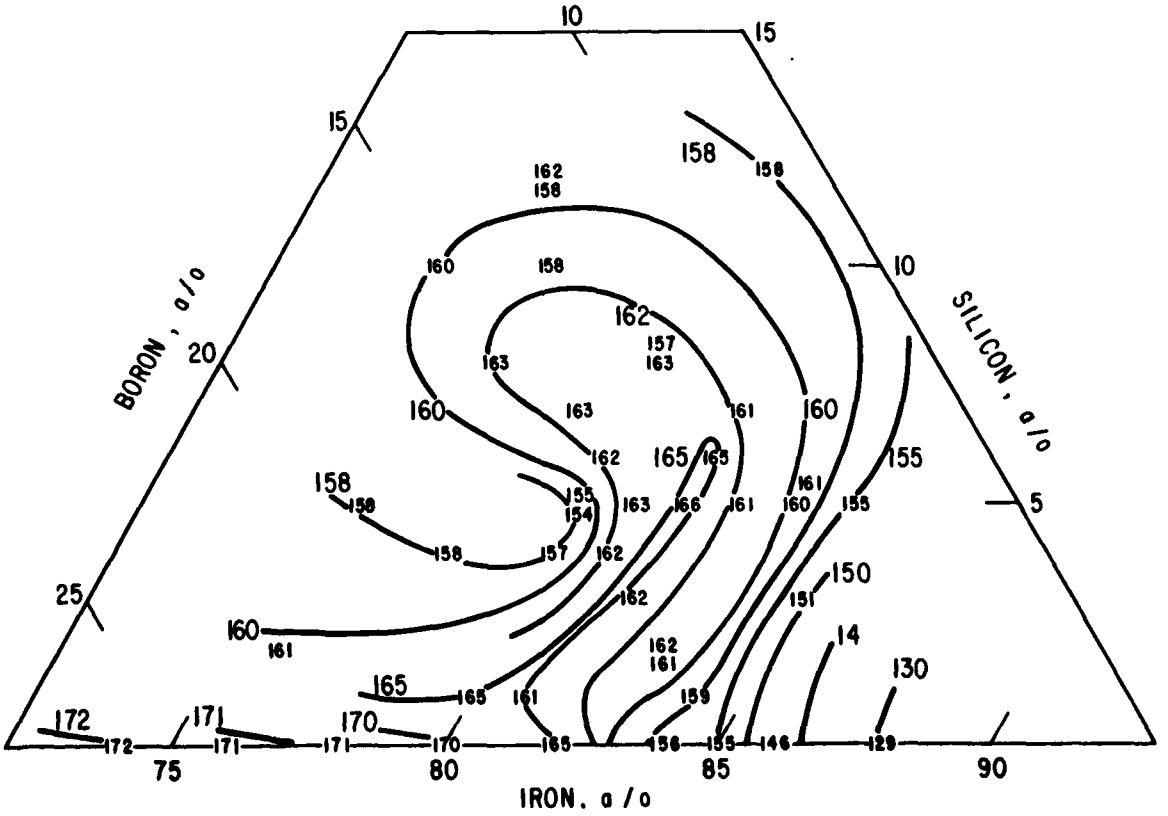

Figure 5. Saturation magnetization at 100 °C for amorphous Fe-B-Si alloys, emu/g.

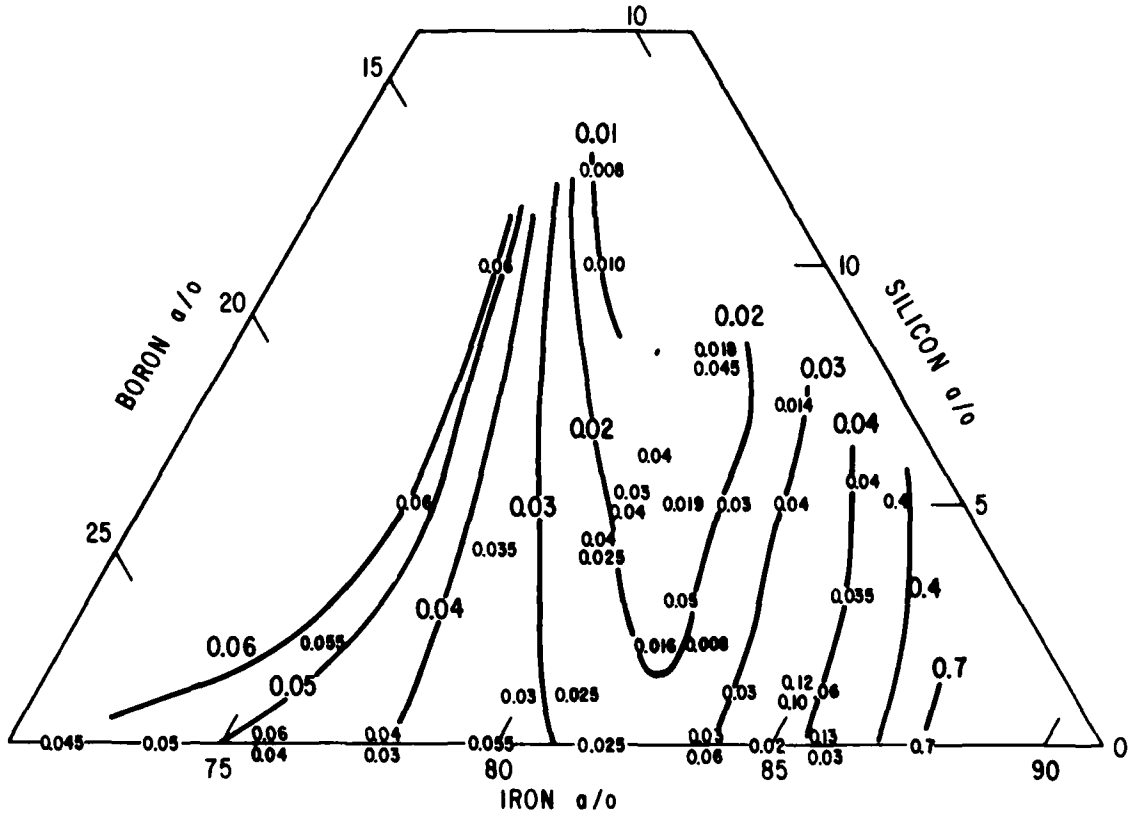

Figure 6. Coercive field for as-cast amorphous Fe-B-Si alloys, Oe.

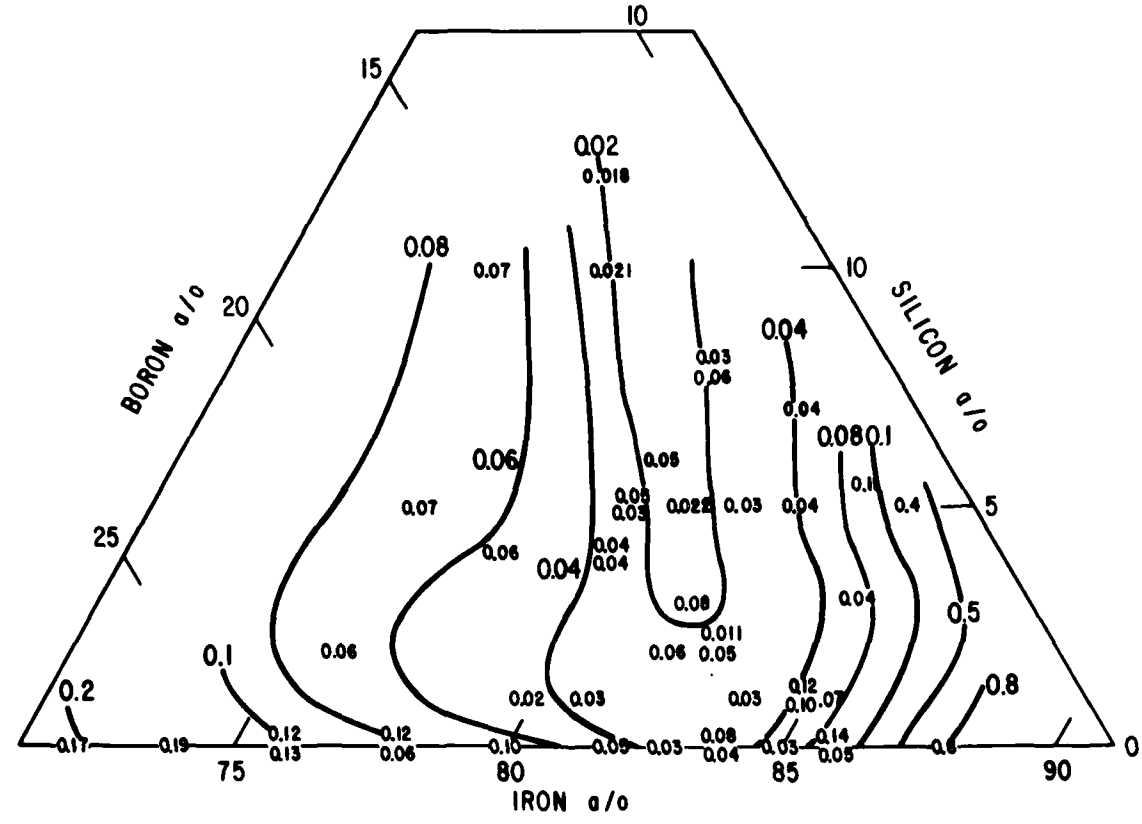

Figure 7. Coercive field for annealed amorphous Fe-B-Si alloys, Oe.

REFERENCES

1. F.E. Luborsky, H.H. Liebermann, J.J. Becker and J.L. Walter, *Rapidly Quenched Metals III, 2* (B. Cantor, ed), The Metals Society, London, p. 188, 1978.
2. K. Fukamichi, M. Kikuchi, S. Arakawa and T. Masumoto, *Solid State Commun., 23*, p. 955, 1977.
3. R. Hasegawa and R. Ray, *J. Appl. Phys., 49*, p. 4174, 1978.
4. R. Hasegawa, R.C. O'Handley, L.E. Tanner R. Ray and S. Kavesh, *Appl. Phys. Lett., 29*, p. 219, 1976.
5. H.H. Liebermann and C.D. Graham, Jr., *IEEE Trans. Magnetics, MAG-12*, p. 921, 1976.
6. K. Hoselitz, *Phys. Status Solidi A, 44*, p. K191, 1977 and private communication.
7. K. Narita, H. Fukunaga and J. Yamasaki, *Japan. J. Appl. Phys., 16*, p. 2063, 1977.
8. T. Masumoto, private communication.
9. A. Inoue, T. Masumoto, M. Kikucki and T. Minemura, *J. Japan Inst. Metals, 42*, p. 294, 1978.
10. J.L. Walter, S.F. Bartram and R.R. Russell, *Met. Trans., 9A*, p. 803, 1978.
11. K. Narita, J. Yamasaki, and H. Fukunaga, *IEEE Trans. Magnetics, MAG-14*, p. 1016, 1978.
12. K. Yamauchi and T. Mizoguchi, *J. Phys. Soc. Japan, 39*, p. 541, 1975.

GENERAL ELECTRIC

General Electric Company
Corporate Research and Development
Schenectady, New York

TECHNICAL INFORMATION SERIES

AUTHOR
Luborsky, FE
Liebermann, HH

SUBJECT
amorphous alloys

NO. 79CRD177
DATE August 1979

TITLE
Stress Relaxation of Iron-Boron Amorphous Alloys

GE CLASS 1
NO. PAGES 2

ORIGINATING COMPONENT
Metallurgy Laboratory

CORPORATE RESEARCH AND DEVELOPMENT SCHENECTADY, N.Y.

SUMMARY

The stress relaxation of Fe_xB_{100-x} alloys for $72 \leqslant x \leqslant 88$ a/o was measured after annealing for 2 hours at 225 °C on ribbons having thicknesses between 15 and 33 μm. Stress relaxation increases approximately linearly with x and with thickness. There was no evidence for any discontinuity in stress relaxation versus x as was previously found for the activation energy for crystallization versus x. This implies that different atomic processes are involved in stress relaxation and in crystallization.

KEY WORDS

amorphous alloys, stress relaxation, iron-boron

INFORMATION PREPARED FOR _____

Additional Hard Copies Available From

Corporate Research & Development Distribution
P.O. Box 43 Bldg. 5, Schenectady, N.Y., 12301

Microfiche Copies Available From

Technical Information Exchange
P.O. Box 43 Bldg. 5, Schenectady, N.Y., 12301

STRESS RELAXATION OF IRON-BORON AMORPHOUS ALLOYS

F.E. Luborsky and H.H. Liebermann

In a previous paper,[1] we reported on the kinetics of crystallization of the series Fe_xB_{100-x}. It was noted that the activation energy, ΔE, and the pre-exponential constant, A, both changed slope at about 81 a/o Fe. This compositional dependence of ΔE and A was attributed to the decrease filling of the holes by B in the Bernal structure as the Fe content increased. The holes are filled for compositions up to 81 a/o Fe, thus resulting in the development of crystal nuclei by a self-diffusion mechanism during annealing resulting in only a small dependence of ΔE and A on composition. For compositions greater than 81 a/o Fe diffusion is aided by the increasing concentration of holes resulting in a large dependence of ΔE and A on composition. It may be expected that other processes that depend on atomic diffusion would also show a change in slope of their diffusion related parameters, for example, in stress-relaxation or in magnetic annealing.

In this note we examine the stress-relaxation behavior. The same samples of amorphous alloys, in the series Fe_xB_{100-x}, were used as reported previously.[1-3] Stress relaxation during annealing for the fixed period of 2 hours at 225 °C was determined as previously described[2] by measuring the radius of curvature of a small hoop, annealing, and then measuring the radius of curvature of the relaxed hoop. A fractional stress relaxation has been defined[2] as

$$F = (\sigma/\sigma_o) = [(r_o/r_a) - (r_o/r_1)]/[1 - (r_o/r_1)]$$

where the ribbon samples with an initial radius of curvature, r_1, are subjected to a strain by placing them in a restraining ring with radius, r_o, which imparts a strain, σ_o.

After annealing, the sample has a residual strain σ. It is then removed from the ring and allowed to relax. Its new radius is then r_a. The results are shown in Figure 1. Sample thicknesses were measured with a micrometer to ± 1.3 μm. The micrometer thickness was used, rather than average thickness, since is was thought that the maximum thickness might be the controlling factor. The average thicknesses were in general about 20% lower than the thickness determined with the micrometer. However, the same trend with composition was observed for the micrometer thickness shown in Figure 1, as was observed for the average thicknesses. Note that two different sample types were used, vacuum cast and air cast. The result of casting in air appears to enhance the stress relaxation. This may be the result of the faster quench rate due to the higher heat transfer provided by the air surrounding the ribbon in contrast to the vacuum, or it may be the result of the rougher surface causing the micrometer thickness to be increased compared to the average thickness.

There is no evidence for any discontinuous behavior around 81% Fe. This implies that the atomic processes involved in stress relaxation are different than those involved in crystallization.

ACKNOWLEDGMENT

The partial support of the Office of Naval Research is gratefully acknowledged.

REFERENCES

1. F.E. Luborsky, H.H. Liebermann and J.J. Becker, *Appl. Phys. Lett.*, 33, 233 (1978).
2. F.E. Luborsky and J.L. Walter, *Materials Sci. Eng.*, 35, 255 (1978).
3. F.E. Luborsky, H.H. Liebermann, J.J. Becker and J.L. Walter, in *Rapidly Quenched Metals III*, B. Cantor, ed., The Metals Soc., London, 1978, Vol. 2, p. 188.

Manuscript received July 13, 1979

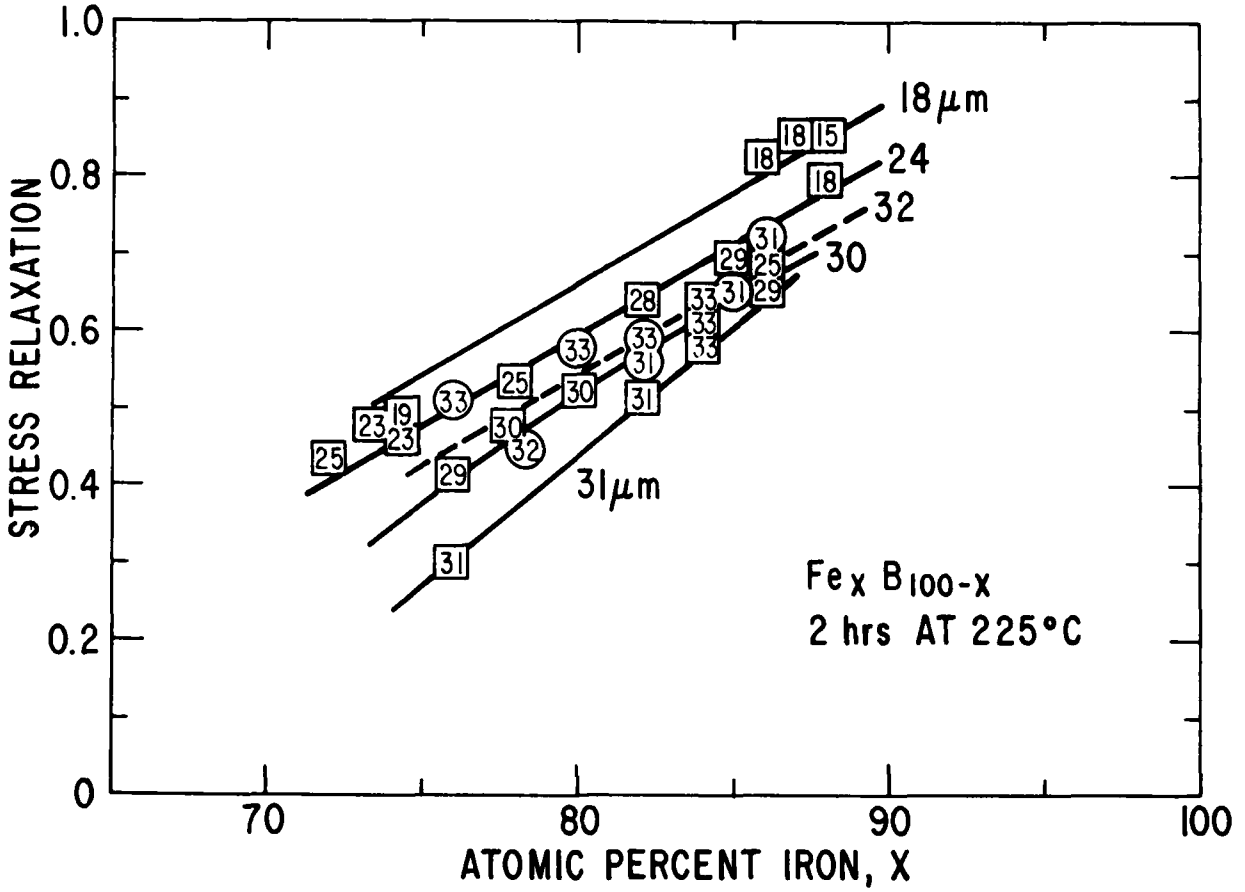

Figure 1. Stress relaxation of Fe-B alloys as a function of iron content after annealing for 2 hours at 225 °C. □ made in vacuum; O made in air. Thicknesses in microns by a micrometer are written in each symbol.

GENERAL ELECTRIC

General Electric Company
Corporate Research and Development
Schenectady, New York

TECHNICAL INFORMATION SERIES

AUTHOR
Luborsky, FE
Walter, JL
Wohlfarth, EP
Liebermann, HH

NO. 79CRD178
DATE October 1979

TITLE
The Effect of Temperature on Magnetic Saturation of Some Amorphous Alloys

GE CLASS 1
NO. PAGES 4

ORIGINATING COMPONENT
Metallurgy Laboratory
CORPORATE RESEARCH AND DEVELOPMENT SCHENECTADY, N.Y.

SUMMARY

The magnetization vs. temperature relation for the amorphous alloys $Fe_{100-x}B_x$, $Fe_{84}B_{16-x}C_x$, $Fe_{80}B_{20-x}Si_x$, $Fe_{80}B_{20-x}Ge_x$ and $Fe_{40}Ni_{40}B_{20-x}P_x$ are reported. Plots of the resulting spin wave stiffness constant D versus the Curie temperature T_c give roughly linear relationships extrapolating to zero D at finite T_c values. These results are discussed on the basis of the itinerant electron model. Neutron scattering values of D are also exhibited for comparison with those obtained here.

SUBJECT
magnetic saturation of amorphous alloys

KEY WORDS
amorphous alloys, magnetic saturation, temperature dependence of saturation

INFORMATION PREPARED FOR _____

Additional Hard Copies Available From
Corporate Research & Development Distribution
P.O. Box 43 Bldg. 5, Schenectady, N.Y., 12301

Microfiche Copies Available From
Technical Information Exchange
P.O. Box 43 Bldg. 5, Schenectady, N.Y., 12301

RD-54 (10/79)

THE EFFECT OF TEMPERATURE ON MAGNETIC SATURATION OF SOME AMORPHOUS ALLOYS

F.E. Luborsky, E.P. Wohlfarth, J.L. Walter, and H.H. Liebermann

INTRODUCTION

Spin wave excitations in ferromagnets have a quadratic dispersion relation for their energy $E(K) = DK^2 + \ldots$ where K is the wave vector and D the spin wave, or exchange, stiffness constant. It was just a few years ago that spin wave resonances were first observed in amorphous ferromagnets.[1] At that time, whether or not spin waves could exist in the amorphous structure with only short range order was interesting from the theoretical point of view. In such amorphous structures the wave vector is not well defined and no simply defined Brillouin zone exists. Kaneyoshi[2] showed that the long wave length spin waves can be clearly and stably defined in an amorphous ferromagnet using the viewpoint that the amorphous magnets have a topologically disordered structure of the type given by the random close packing of atomic spheres.

From a more practical viewpoint, Hatta and Egami[3] reported that the high room temperature saturation magnetization of Fe-B-C alloys is, in large part, the result of the decrease in the slope of the magnetization vs. temperature curve as the content is increased. They reported values of β in the low temperature spin wave approximation

$$M(T)/M(O) = 1 - \beta(T/T_c)^{3/2} \qquad (1)$$

of 0.43 for $Fe_{86}B_9C_5$ compared to 0.65 for $Fe_{86}B_{14}$ and 0.55 for $Fe_{84}B_{10}C_6$ compared to 0.63 for $Fe_{84}B_{16}$. Hatta and Egami[3] and Fukamichi et al.[4] both reported some limited results for β of some $Fe_{100-x}B_x$ alloys. However, Kazama et al.[5] reported an increase in D with x for the entire series and showed that D varied linearly with T_c. They infer from these results the character of the Fe-Fe exchange interactions.

Thus it was of interest to examine the low temperature behavior of other amorphous alloy systems such as the Fe-B binary alloys as well as Fe-B alloys containing C, Si, Ge and Fe-Ni-B-P and to try to establish some degree of systematics of the spin wave stiffness, as dependent on the alloy composition.

EXPERIMENTAL PROCEDURE

Magnetizations at room temperature and below were determined in a vibrating sample magnetometer to a maximum field of 20 kOe on specimens about 0.5 cm long and about 0.1 cm wide. Results were extrapolated to infinite field using a $1/H^2$ law. Magnetization, M(T), above room temperature was determined using a force balance made up of a Dupont 951 thermogravimetric recording balance with a Dupont 990 thermal analyzer control unit. The furnace was non-inductively wound and fitted with a large permanent magnet to produce a field gradient together with a field of 225 Oe along the length of 1-cm-long ribbons. The samples were heated at 20 deg/min. The Curie temperature, T_c, was determined as the intersection of M(T) with the temperature axis. The magnetization at 0 K, M(O), was determined by extrapolating to 0 K from 77 K and above on a $T^{3/2}$ scale.

TEMPERATURE DEPENDENCE OF M_s

The M(T) vs. T curves for the Fe-B amorphous alloys as the boron content increases are shown in Figure 1. We have calculated the values of β from the data between 77 and 300 K, using Eqn. (1). The use of magnetization results up to room temperatue may be justified on the basis of past experience[3,6-8] which showed that Eqn. (1) is valid for amorphous alloys to much higher temperatures than for crystalline alloys, in fact up to $T/T_c \cong 0.5$; i.e., near room temperature.

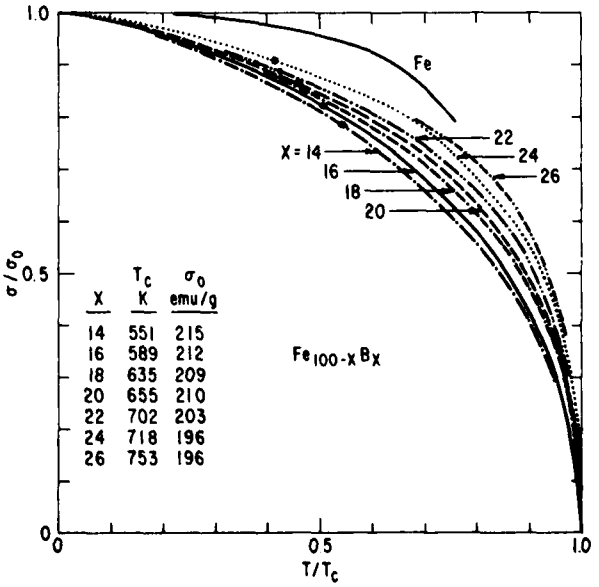

Figure 1. Reduced magnetization-temperature curves for $Fe_{100-x}B_x$ alloys compared to crystalline Fe. The * indicates room temperature.

Manuscript received July 13, 1979

There may be other contributions to M(T) for these materials, however, arising from itinerant ferromagnetism ($\sim T^2$), from thermal expansion effects and from the amorphicity itself, when compared to equivalent crystalline alloys. The values of β are shown in Figure 2. This trend is consistent with previously reported results[3,4] for the Fe-B alloys. Note that the values of β for the two extreme compositions are off the trend line. This is due to the fact that these two samples showed evidence for the presence of some slight crystallinity.[9]

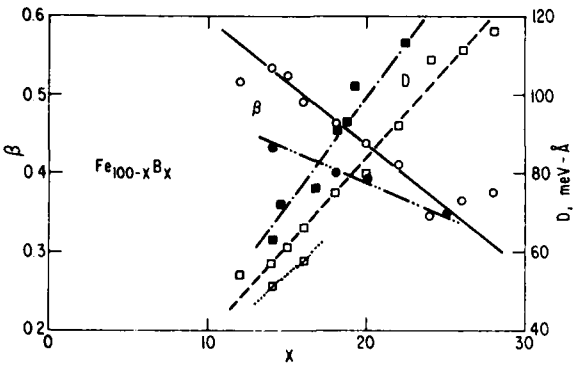

Figure 2. Slope of the spin wave equation β and the exchange stiffness constant D for $Fe_{100-x}B_x$ alloys. ■ from ref. 5; □ from ref. 3; O from ref. 11.

The magnetization vs. temperature curves for various Fe-B-X alloys were also determined. Where more than one sample was tested, the maximum deviation from the curve was ±3% at $T/T_c \cong 0.7$. The results for β are shown in Figure 3(a) for Fe-B-C, Fe-B-Si, Fe-B-Ge and Fe-Ni-B-P alloys. In contrast to the decrease in β by C, Si and Ge, the replacement of B by P in the $Fe_{40}Ni_{40}B_{20-x}P_x$ alloys results in an increase in β.

DISCUSSION

The Exchange Stiffness

The value of β can be expressed in terms of D by the equation[10]

$$\beta = (g\mu_\beta/M_o)\,(k/4\pi D)^{3/2}F_{3/2}(T) \qquad (2)$$

where g = 2.1, M_o = magnetization at 0 K, and $F_{3/2}(T)$ = Bose-Einstein integral function = 2.61. The values of D calculated from (2) are displayed in Figures 2 and 3(b). Note in Figure 2 that our values for D appear to fall between the previously reported values,[3,5] and the β values are close to values derived from Mossbauer hyperfine field measurements.[11] The values of M_o were obtained from the measured values (emu/g) using the densities of the various alloys. This density was calculated by first calculating the packing fraction vs. Fe content for the Fe-B alloy series using the measured densities of Hasegawa and Ray.[12] Then the densities of the various ternary alloys were calculated using these packing fractions for each Fe content together with the tetrahedral covalent radii of B, Si, Ge, and P as previously described.[10] Excellent agreement was obtained between these calculated densities and some measured densities in the Fe-B-C system[13] and for some few measured densities in the Fe-B-Si system.

The correlation between D and T_c found by Kazama et al.[5] for the Fe-B alloys was confirmed in this work as shown by closed symbols in Figure 4, and appears to hold also for most of the other Fe-B-X alloys as well as Fe-Ni-B-P. The values of D obtained here from M(T) data may be supplemented by values obtained from neutron scattering measurements[6-8,14-19] shown in Figure 4 by open symbols. It appears that the two sets of data agree reasonably well for the Fe-Ni-B-P alloys but not for the Fe-B-X alloys. Differing D values from magnetization and neutron sources also occur for crystalline materials such as nickel;[20] this effect is not fully understood. Figure 4 also shows a few values of D from neutron scattering for amorphous Co-X.

The general trend of these D vs. T_c plots seems rather clear. There are roughly three sets of data, giving an approximately linear dependence and corresponding to:

1. Fe-B and Fe-B-X,
2. Fe-Ni-B-P and
3. Co-X

in increasing order of D. For [1.] extrapolation of the curve to zero D occurs at T_c about 380 K, for [2.] at about 200 K and for [3.] at about 0 K. It may be noted that the value of T_c for "amorphous iron," obtained by extrapolating the data for $Fe_{100-x}B_x$ as $x \rightarrow 0$, is about 300 K.[9]

The correlation between D and T_c has been discussed for the itinerant electron model by Katsuki and Wohlfarth.[21] They obtained linear relationships between these two quantities for *weak* itinerant ferromagnets with slopes determined by the effective intra-atomic coulomb interaction and extrapolating to zero D at zero T_c. The observed data in Figure 4 also give such linear relationships but with the same slopes and with most of the results not extrapolating to zero. It has been suggested[22] that amorphous Fe-B alloys may be regarded as *strong* or almost strong itinerant ferromagnets. For these the D vs T_c curves of Ref. 21 are no longer strictly linear and the values of D *decrease* with increasing T_c so as to extrapolate to zero D at a finite T_c. In this case also the experimental data are thus only partially explained by the calculations of Ref. 21. These early calculations, however, were based on a very simple band structure and it can only be claimed that they already contain the germs of an explanation of the present complicated observations. If the extrapolation of the data to zero D at finite T_c is thus a real effect in the sense of this calculation; i.e., in the sense of spin wave mode softening, it may give

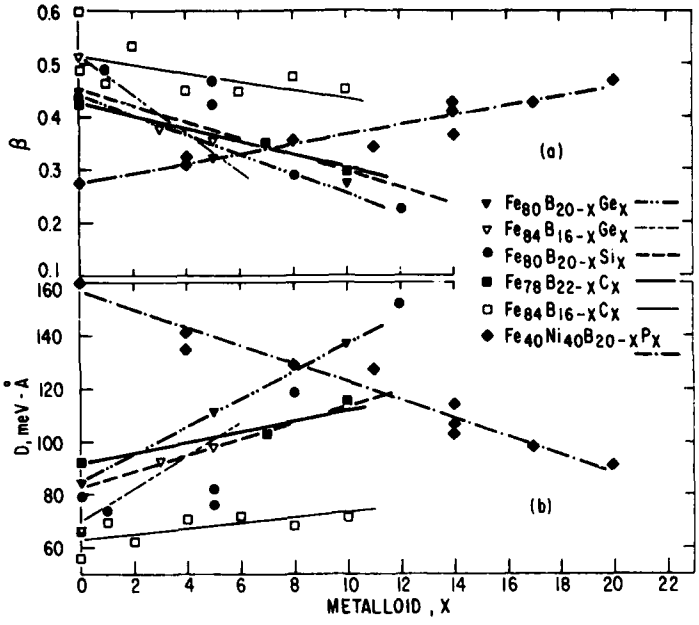

Figure 3. **(a) Slope of the low temperature spin wave equation as a function of metalloid content for various amorphous alloys. (b) The exchange stiffness constant for the same alloys as in (a).**

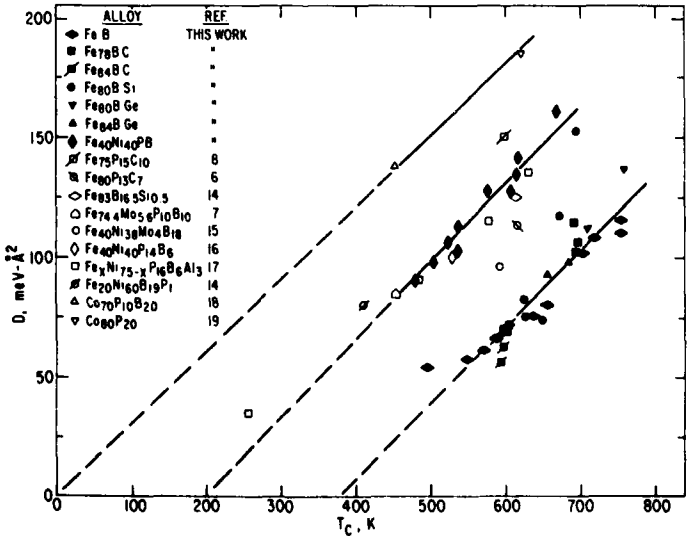

Figure 4. **The exchange stiffness constant D as a function of Curie temperature for various alloys. Solid and broken lines drawn through points to guide the eye. Closed symbols, data from present measurements; open symbols, data from neutron measurements.**

a valuable hint as to the nature of magnetism in amorphous materials.

ACKNOWLEDGMENTS

The ribbons were prepared by W. Rollins. The measurements of magnetization were made by H. Patchen under the direction of I.S. Jacobs and by J.J. Becker. The high temperature measurements were made by N. Marotta. The densities were calculated by J. Gillespie and measured by D.L. Martin. The partial support of the Office of Naval Research is gratefully acknowledged. E.P. Wohlfarth thanks the General Electric Company for the award of a Visiting Fellowship.

REFERENCES

1. T. Kaneyoshi, *J. Phys.* C5 (1972) 5304.
2. T. Kaneyoshi, *J. Phys. Soc. of Japan* 45 (1978) 1835.
3. S. Hatta and T. Egami, *J. Appl. Phys.* 50 (1979) 1589.
4. K. Fukamichi, M. Kikuchi, S. Arakawa and T. Masumoto, *Solid State Comm.* 23 (1977) 955; K. Fukamichi, H. Hiroyoshi, M. Kikuchi and T. Masumoto, *J. Magnetism Magn. Mat.* 10 (1979) 294.
5. N.S. Kazama, M. Mitera and T. Masumoto, in *Rapidly Quenched Metals III*, Vol. 2, B. Cantor, ed. (The Metals Soc., London, 1978) p. 164.
6. N. Kazama, T. Masumoto and H. Watanabe, *J. Phys. Soc. Japan* 37 (1974) 1171.
7. J.D. Axe, G. Shirane, T. Mizoguchi and K. Yamauchi, *Phys. Rev.* B15 (1977) 2763.
8. C.L. Chien and R. Hasegawa, *Phys. Rev.* B16 (1977) 2115.
9. F.E. Luborsky, H.H. Liebermann, J.J. Becker and J.L. Walter, *Rapidly Quenched Metals III*, Vol. 2, B. Cantor, ed. (The Metals Soc., London, 1978), p. 188.
10. F.E. Luborsky, in *Ferromagnetic Materials*, E.P. Wohlfarth, ed. (North-Holland Publ. Co., 1979).
11. C.L. Chien, D. Musser, E.M. Gyorgy, R.C. Sherwood, H.S. Chen, F.E. Luborsky and J.L. Walter, *Phys. Rev.*, to appear.
12. R. Hasegawa and R. Ray, *J. Appl. Phys.* 49 (1978) 4174.
13. F.E. Luborsky, J.J. Becker, J.L. Walter and D.L. Martin, *IEEE Trans. Magnetics*, to appear.
14. J.J. Rhyne, J.W. Lynn, F.E. Luborsky and J.L. Walter, *J. Appl. Phys.* 50 (1979) 1583.
15. R. Krichnan, S. Prasad and K. Branski, *Proc. Joint Intermag-MMM Conf.*, 1979.
16. J.W. Lynn and J.J. Rhyne, to appear.
17. J.A. Tarvin, G. Shirane, R.J. Birgeneau and H.S. Chen, *Phys. Rev.* 17 (1978) 241, and *AIP Conf. Proc.* 34 (1976) 313.
18. J.R. McColl, D. Murphy, G.S. Cargill and T. Mizoguchi, *AIP Conf. Proc.* 29 (1976) 172.
19. H.A. Mook, N. Wakabayashi and D. Pan, *Phys. Rev. Lett.* 34 (1975) 104.
20. E.P. Wohlfarth, in *Ferromagnetic Materials*, E.P. Wohlfarth, ed. (North-Holland Publ. Co., 1979).
21. A. Katsuki and E.P. Wohlfarth, *Proc. Roy. Soc.* A295 (1966) 182.
22. E.P. Wohlfarth, *J. Magnetism Magn. Mat.* 10 (1979) 120.

GENERAL ELECTRIC

General Electric Company
Corporate Research and Development
Schenectady, New York

TECHNICAL INFORMATION SERIES

AUTHOR	SUBJECT	NO.
Luborsky, FE Becker, JJ	magnetic properties of amorphous alloys	79CRD134
		DATE June 1979
TITLE Strain Induced Anisotropy in Amorphous Alloys and the Effect of Toroid Diameter on Magnetic Properties		GE CLASS 1
		NO. PAGES 17
ORIGINATING COMPONENT	Metallurgy Laboratory	CORPORATE RESEARCH AND DEVELOPMENT SCHENECTADY, N.Y.

SUMMARY

The magnetic properties of toroids wound from amorphous Fe-B-Si alloy ribbons has been examined as a function of toroid diameter and for ribbon widths from 0.1 cm to 2.5 cm. For the smallest ribbon widths, as the diameter decreased from 20 cm to 1 cm, the magnetic coercivity before annealing increased by a factor of ten and the remanence-to-saturation ratio decreased from ~0.7 to less than 0.4. After annealing in a field, the coercivity still increased with decreasing diameter by a factor of ten and the ratio of remanence-to-saturation dropped from ~0.9 to ~0.45. The losses after annealing similarly increased by a factor of ten and the permeability decreased. These lowest losses, obtained from large diameter toroids, are below those of the best commercial alloys (Supermalloy, 4-79 Mo-Permalloy and Deltamax) and are well below any previously reported amorphous alloy. Wider tapes, 1 cm and 2.5 cm in width of similar Fe-B-Si compositions, were found to have properties essentially independent of their diameter. This difference in behavior between narrow and wide tapes can be understood on the basis of their differences in strain distribution. The approach to saturation after annealing was found to improve with increasing nickel in the amorphous alloys $Fe_xNi_{80-x}B_{20}$. This is attributed to the decrease in magnetostriction which decreased the anisotropy arising from strain induced ordering. This assumption was confirmed when it was noted that the approach to saturation became much easier when the inner half of the thickness of an annealed toroid tape was etched away removing material with annealed in strain induced ordering. The impairment in properties of toroids with decrease in diameter is thus attributed to the increase in the strain induced ordering anisotropy. In order to eliminate the effect of toroid diameter on the magnetic properties we wound the toroids with sufficient tension to overcome the compressive forces developed in the tapes due to their radius of curvature. Rather than improving the properties, winding with tension significantly deteriorated the properties. This is believed due to the radial forces introduced by the winding tension. The effects of tensional loads and of compressive loads on the surface of straight ribbons were studied and confirmed the results obtained in the toroids.

KEY WORDS

amorphous alloys, magnetic properties, induced anisotropy, toroids

INFORMATION PREPARED FOR _____

Additional Hard Copies Available From

Corporate Research & Development Distribution
P.O. Box 43 Bldg. 5, Schenectady, N.Y., 12301

Microfiche Copies Available From

Technical Information Exchange
P.O. Box 43 Bldg. 5, Schenectady, N.Y., 12301

INTRODUCTION

In conventional crystalline alloy tapes the diameter of the toroid has no effect on the magnetic properties. However, it has recently been found, both in our laboratory and elsewhere [1], that the magnetic properties of amorphous alloys depend strongly on diameter. Fujimori et al [1] working with 2 mm wide $Fe_{72}Co_8Si_5B_{15}$ amorphous alloy annealed in a magnetic field, reported a decrease in d.c. coercivity, from ∿0.065 Oe down to 0.035 Oe on increasing the toroid diameter from ∿1.7 cm to 4.5 cm. Over the same size range the loss per cycle at B_{max} = 1000G and 50 Hz decreased from ∿9.5 mW-sec/kg to 2.7 mW-sec/kg. They attributed the effect of diameter on the magnetic properties to the lack of complete stress relief.

On examining the literature for results on magnetic remanence-to-saturation ratio, M_r/M_s, for toroids it has been found that the highest value reported for high magnetization alloys, i.e. iron-rich alloys, is 0.77 [2,3]. This was for 2 mm wide $Fe_{80}B_{20}$ ribbon, wound into a 3.7 cm diameter toroid, and annealed in a field. More typically values for this alloy, as well as for $Fe_{80}P_{14}B_6$, are about 0.5 [4]; but these were for 1.4 cm diameter toroids. Only alloys with considerable nickel, such as $Fe_{40}Ni_{40}P_{14}B_6$ and $Fe_{40}Ni_{40}B_{20}$, show larger values of M_r/M_s. For example, values of 0.85 [4] to 0.90 [5] have been reported for 1.4 cm diameter toroids of $Fe_{40}Ni_{40}P_{14}B_6$ amorphous alloy. All of these results are for narrow, 1-2 mm wide, ribbons. On the other hand, results reported on measurements on straight samples, after stress relief anneal, all show very square hysteresis loops. For example, Fujimori [1] reported values of above 0.9 for annealed $Fe_{72}Co_8B_{15}Si_5$ and Luborsky et al [6] reported values for $Fe_{40}Ni_{40}P_{14}B_6$ also well above 0.9. Thus, it is clear that there is a problem with the M_r/M_s and the approach to saturation of toroids of high saturation amorphous alloys.

Manuscript received 5/3/79.

In this paper we have studied the stress relaxation of our Fe-B-Si amorphous alloys and the effect of diameter on the properties using diameters from 1 cm to 20 cm. We show that stress relaxation of the winding stress is complete and yet there is still a large effect of diameter on the properties of narrow ribbons but not for wide ribbons. We show that the effect of diameter on the properties is the result of the stress induced anisotropy which develops during the anneal.

EXPERIMENTAL

Amorphous alloys of various Fe-B-Si compositions were prepared by rapid solidification from the melt [7]. Stress relaxation was determined by measuring the radius of a relaxed ribbon after annealing in the form of a tight coil [8]. All of the samples used in this work were found to be at least 95 percent stress relieved before crystallization was found to start. Static hysteresis loops were obtained using an integrating fluxmeter. Hysteresis losses and permeability were measured using the volt-ampere-phase shift method as previously described [9]. All annealing and cooling was carried out in a 35 Oe field under nitrogen unless specified otherwise. The toroids were prepared by winding about 10-15 turns of amorphous tape into an open aluminum, aluminum bronze, or lava coil form. Twenty-five to fifty turns of wire were then wound around the coil form for a drive field and the same number for a sense winding. The narrow straight samples were 1 and 2.5 mm wide and 10 cm long, the wide straight samples were 1 and 2.5 cm wide and 35 cm long. These were measured in a long solenoid with a 3000 turn sense coil in the center.

RESULTS AND DISCUSSION

(a) Coercive field and remanent magnetization

The results of measuring the coercive field and the magnetization ratios from the static hysteresis loop are shown in Figs. 1 and 2 as a function of

inverse diameter using anneal temperature as a parameter. These ribbons were about 1 mm wide. The remarkable increase in H_c of over a factor of ten as the diameter decreases is most noteworthy. Note also that the results for the straight sample form a natural extension of the results for the toroids. The anneal appears to reduce H_c by a constant percentage of the initial value independent of the diameter.

A similar dependence on diameter is shown by the magnetization-to-saturation magnetization ratio, M_H/M_S. This is shown in Fig. 2 as a function of anneal temperature. Note also that an annealed toroid of Supermalloy had a much higher value of magnetization in 10 Oe to saturation, M_{10}/M_S, than the amorphous alloys of similar diameter although its M_r/M_S was roughly equivalent to the values for the amorphous alloys. This difference is believed due to the fact that the magnetostriction of the Supermalloy is essentially zero while the magnetostriction of the amorphous alloys has the large value of $\sim 35 \times 10^{6}$. Very similar coercivity and magnetization diameter results were obtained on another sample of similar composition and width, namely $Fe_{82}B_{15}Si_3$ with a width of 2.5 mm. In this somewhat wider sample the coercivity changed by a smaller amount; going from 0.05 Oe for the straight sample to 0.12 Oe for the 1.1 cm diameter sample after annealing for 2 hours at 325°C. This compares to 0.010 Oe for the straight sample to 0.15 Oe for the 1.1 cm diameter sample for the narrower specimen. Similarly, the M_r/M_S changed from 0.83 for the straight sample to 0.38 for the 1.1 cm diameter sample after annealing for 2 hours at 325°C. This compares to a change from 0.93 for the straight sample down to 0.42 for the 1.1 cm diameter sample for the narrower specimen. Thus, although the changes in the wider 2.5 mm tape are somewhat smaller than for the 1 mm tapes the changes are qualitatively the same.

In contrast to the above, wide tapes showed no deterioration in properties on winding toroids. Comparisons were made between straight samples and samples wound onto 4.3 cm diameter toroids. Fifteen different 1 cm wide samples were prepared from $Fe_{81.5}B_{14.5}Si_4$. Nine different batches of 2.5 cm wide METGLAS^R 2605B alloy were obtained from Allied Chemical Company. For all twenty-four samples measured both before and after annealing the H_c increased on winding the toroid an average of 35% with σ = 43%. Similarly, the magnetization at 1 Oe, M_1, showed an increase of only 12% with σ = 33%. These changes are much smaller than for the narrow ribbons and in fact the small increase in M_1 is in the reverse direction from that expected.

The comparative behaviors of narrow and wide strips can be qualitatively understood in the following way. When a flat ribbon is bent into a cylinder, the inside surface is in compression and the outside in tension. On the compression side, if the magnetostriction is positive, the ribbon axis becomes a hard direction of magnetization. The material on the compression side will tend to expand normal to the ribbon axis, both in the surface and normal to it, in accordance with Poisson's ratio. However, the magnetization will tend to lie in the tape, transverse to the axis, rather than point out of the surface, which would require an additional magnetostatic energy. The slow approach to saturation then comes from the necessity of rotating this transverse magnetization into the axis. In a wide strip, the transverse expansion of the material in accordance with Poisson's ratio is not possible due to the plane strain conditions. Thus, there is no transverse strain to interact with the magnetostriction. There is still tensile strain normal to the compression surface, so this normal becomes the easiest direction and the magnetization points out of the surface. Rotating it into the applied field direction is easier because of the accompanying reduction in magnetostatic energy, so the approach to saturation

is more rapid. Preliminary domain studies by J. D. Livingston appear to confirm this differing behavior of the magnetization in narrow and wide ribbons.

(b) Losses and permeability

It would be expected that the large increase in coercive field with decrease in toroid diameter would result in a corresponding increase in losses and decrease in permeability. Indeed the losses have been found to increase by an amount equivalent to the increase in H_c, i.e. by more than a factor of ten. These results are shown in Fig. 3 as a function of inverse diameter and measurement frequency. Note that the results are for the two somewhat different Fe-B-Si alloys ($Fe_{83}B_{15}Si_2$ about 1 mm wide and $Fe_{82}B_{15}Si_3$ about 2.5 mm wide) and for two different stress relief anneals (2 hours at 300°C and at 325°C) both in a magnetic field. The results are reported for B_m = 1kG. In a similar manner the impedance permeability measured for ΔB = 100G decreased by a factor of greater than three on increasing the diameter. These results are shown in Fig. 4 for the same two alloys but the results of the two anneal temperatures were averaged together since, as in Fig. 3, they show little or no trend between these two anneal temperatures.

We now compare the lowest loss toroid of $Fe_{83}B_{15}Si_2$, i.e. the 20 cm diameter, to conventional materials in Fig. 5. This comparison is made for measurements at 50 kHz on 50μ thick alloys of Fe-3.2% Si, 50-50 NiFe, 4-79 Mo-Permalloy and Supermalloy taken from an Arnold Engineering Co. catalog [10]. The same relative positions of the curves is observed at other frequencies. The amorphous alloy is more than a factor of two below the catalog values of the best metallic tapes available today. See Table I for comparison of other properties. This is the first time that values for losses of amorphous alloys are reported that are equal to or less than for the Permalloys. In Fig. 6 we compare this 20 cm diameter toroid result to other reported curves for amorphous alloys wound to smaller diameters and to Fe-3.2% Si alloys of various thicknesses.

The 20 cm diameter toroid is a factor of ∿4 times lower than the best amorphous alloy previously reported; namely the zero magnetostrictive $Fe_3Co_{72}P_{16}B_6Al_3$. It is over a factor of ten lower than the high magnetization alloy $Fe_{80}B_{20}$ previously reported from measurements on smaller diameter toroids.

(c) Effect of Fe/Ni on approach to saturation

In order to determine if the magnetostriction has an influence on the approach to saturation of the small 1.4 cm diameter toroids we measured a number of ∿1 mm wide samples in the series $Fe_xNi_{80-x}B_{20}$. In this series of alloys the magnetostriction falls from about 32×10^{-6} to 3×10^{-6} in going from $Fe_{80}B_{20}$ to $Fe_{20}Ni_{60}B_{20}$ [11,12]. The results of the approach to saturation are summarized in Fig. 7 by plotting M_{10}/M_s vs Fe concentration for the toroids and for straight samples. In all cases the samples were stress relieved by annealing in a field of 5 Oe for two hours at temperatures from 320 to 345°C [8]. The increasing difficulty of saturating the toroids with increase in iron is apparent as compared to the straight samples. This must be related to the magnetostriction but since the samples are all stress relieved it cannot be the result of a strain-magnetostriction interaction anisotropy. Note also that samples cast in vacuum behave essentially the same as samples cast in air.

(d) Effect of etching

In order to determine whether the effect of the iron content on the approach to saturation is due to a strain-magnetostriction interaction or to a strain induced ordering, a 1.4 cm diameter toroid made from ∿2 mm wide ribbon was annealed, removed from the core box, and the outer surface of the ribbon protected with acid resistant masking tape. The ribbon was then etched to remove approximately 50% from its inner surface, the masking tape removed and the ribbon reinserted into the core box and remeasured. By this procedure the inner half of the thickness of the ribbon was removed after the ribbon was

annealed as a small diameter toroid. The result of this procedure is shown in Fig. 8. Note that there is no change in the high field approach to saturation beyond about 15 Oe but below 15 Oe the approach to saturation is much sharper after etching. Thus, we conclude that we have removed material with an unfavorably oriented anisotropy.

(e) Toroids wound under tension

It was hoped that by winding toroids with sufficient tension to overcome the maximum compressive stress introduced by the radius of curvature that the properties would improve. The toroids were wound in two ways. The first one, using the alloy $Fe_{81.7}B_{15}Si_3Al_{0.1}C_{0.2}$, about 2 mm in width, was wound on the outside of a ceramic core form and the outer turn glued down to hold the windings in tension. The next two toroids were wound on the outer surface of the aluminum-bronze core form shown in cross-section in Fig. 9a. The drawing is not to scale and ten turns of tape were used rather than the one turn shown. The end was spot welded by inserting a copper strap under the last turn under the support rod. Two different alloys were used; one was from Allied Chemical Co., METGLAS^R 2605B, 2.5 cm wide, the other was $Fe_{81.5}B_{14.5}Si_4$, 1 cm wide.

The results are shown in Figs. 9. Note first of all that in the as-wound condition, the coercivity shown in Fig. 9(a) of all three samples, increases with increase in tension. This is the reverse of that found for straight strips as shown in Fig. 10. However, M_r/M_s shown in Fig. 9(b), M_1/M_s shown in Fig. 9(c), and M_{10}/M_s for as-wound toroids, all rise with increase in tension although at a very slow rate compared to the results on the straight ribbon. After annealing the H_c still increases with increase in tension. However, now M_r/M_s, M_1/M_s and M_{10}/M_s all decrease with increase in tension. This decrease is believed to be due to the compressive surface forces developed on winding the toroids. In addition, it may be due to compressive forces developed on

cooling from the high temperature with stress applied. This increase in H_c and decrease in M_H/M_s was also observed in the straight strips annealed with tension. This is shown in Fig. 10 also. Thus, the improvement hoped for by applying stress during winding a toroid has not been realized.

(f) Effect of Stress on Straight Ribbons

In order to confirm that this alloy has a positive magnetostriction we tested a straight strip. The results shown in Fig. 10 show a drop in coercivity and increase in squareness for a relatively small application of tension. These results are similar to results previously reported [13]. These ribbons were then annealed by applying a static load on the end of the ribbon. The load was then removed before testing. These annealed samples now show a reverse trend with applied tension compared to the as-cast samples. These results suggest that compressive strains are introduced after the anneal by removing the loading, thus causing transverse rotation on the magnetization.

A compressive load was also applied on the face of the same ribbon in order to simulate the forces developed on winding a toroid with applied tension. This was done by simply clamping a 1.6 cm length in the center of the 35 cm long ribbon between two thick copper plates using two brass bolts. A 0.030 cm thick lead sheet was inserted to equalize the load distribution. Results for the annealed specimen are shown in Fig. 11. Note the large drop in remanence with application of face pressure. Similar results were obtained on an as-cast sample. With removal of the stress, by loosening the bolts, the "relaxed" curve was again obtained. These results of compressive loading can be interpreted as the rotation of the magnetization transverse to the compressive loading direction but randomly oriented in the plane of the tape.

CONCLUSIONS

The effect of diameter of the toroid on the magnetic properties has clearly been shown to be due to a strain induced ordering resulting from the stresses

introduced by the radius of curvature and influenced by the ribbon width. We thus conclude that the stress pattern introduced during the original quenching to form the amorphous ribbon will also influence the stress induced ordering and thus the resultant magnetic properties developed after annealing.

ACKNOWLEDGMENTS

We wish to acknowledge the work of A. C. Rockwood, R. Laing and H. H. Liebermann in preparing our samples; the help of J. J. Gillespie in the measurement and calculation of losses and in the winding of the toroids under tension; and the discussions with D. Lee and J. Livingston concerning the effects of bending stresses. The partial support of the Office of Naval Research is gratefully acknowledged.

Table I. Magnetic Properties of Large Diameter Amorphous Alloy Core Compared to Supermalloy

	20 cm diam, $Fe_{82}B_{15}Si_3$		Supermalloy
	2 hrs at 300°C	2 hrs at 323°C	Annealed
H_c, Oe	0.031	0.058	0.005
M_r/M_s	0.77*	0.82*	0.59
$4\pi M_s$, kG	16	16	8.2
loss, mw/cm^3			
@ 1kG, 100 Hz	0.0025	0.0035	0.0029
1 kHz	0.12	0.095	0.14
10 kHz	3.0	4.0	7.5
100 kHz	90.	80.	400.
μz			
@ΔB=100G, 100 Hz	8100*	7000*	65,000
1 kHz	7300*	6000*	50,000
10 kHz	5600*	4900*	19,000
100 kHz	3800*	3100*	4,400

*interpolated

REFERENCES

1. H. Fujimori, T. Kato, T. Masumoto and H. Morita, Rapidly Quenched Metals III, edited by B. Cantor, The Metals Society, London 1978, vol. 2, p. 240.
2. R. C. O'Handley, L. I. Mendelsohn, R. Hasegawa, R. Ray and S. Kavesh, J. Appl. Phys., vol. 47, p. 4660, 1976.
3. R. Hasegawa, R. C. O'Handley and L. I. Mendelsohn, AIP Conf. Proc., vol. No. 34, p. 298, 1976.
4. F. E. Luborsky, Amorphous Magnetism II edited by R. A. Levy and R. Hasegawa, Plenum Press 1977, p. 345.
5. F. E. Luborsky, R. O. McCary and J. J. Becker, Rapidly Quenched Metals, Edited by N.J. Grant and B.C. Giessen, MIT Press, Cambridge, Mass. 1976, p. 467.
6. *F. E. Luborsky, J. J. Becker and R. O. McCary, IEEE Trans. Magnetics,* vol. MAG-11, p. 1644, 1975.
7. H. H. Liebermann and C. D. Graham, Jr., IEEE Trans. Magnetics, vol. MAG-12, p. 921, 1976.
8. F. E. Luborsky and J. L. Walter, Materials Science and Eng., vol. 35, p. 255, 1978.
9. F. E. Luborsky, J. L. Walter and H. H. Liebermann, IEEE Trans. Magnetics, vol. MAG-15, p. 909, 1979.
10. Arnold Engineering Co., Catalog TC-101B, 1972.
11. F. E. Luborsky, J. Magnetism and Mag. Materials, vol. 7, p. 143, 1978.
12. R. C. O'Handley, Solid State Comm., vol. 22, p. 485, 1977.
13. T. Egami, P. J. Flanders and C. D. Graham, Jr., Appl. Phys. Lett., vol. 26, p. 128, 1975.

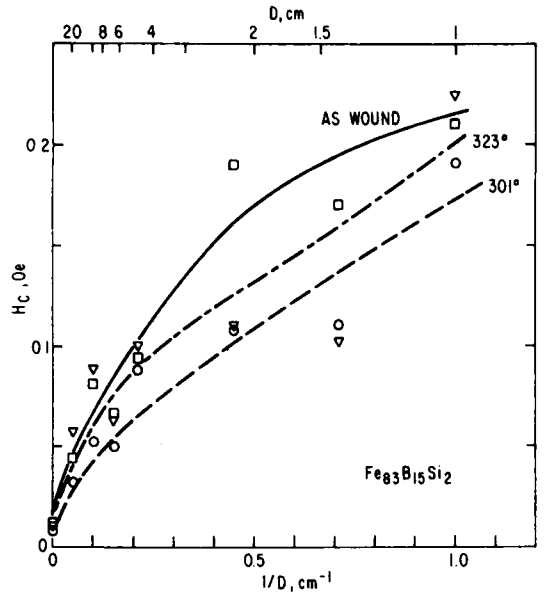

Fig. 1 Coercive field as a function of diameter of the toroid for samples prepared from ∿1 mm wide ribbons of $Fe_{83}B_{15}Si_2$, as-wound and then annealed for 2 hrs. at 301°C and 323°C in a circumferential field = 20/D.

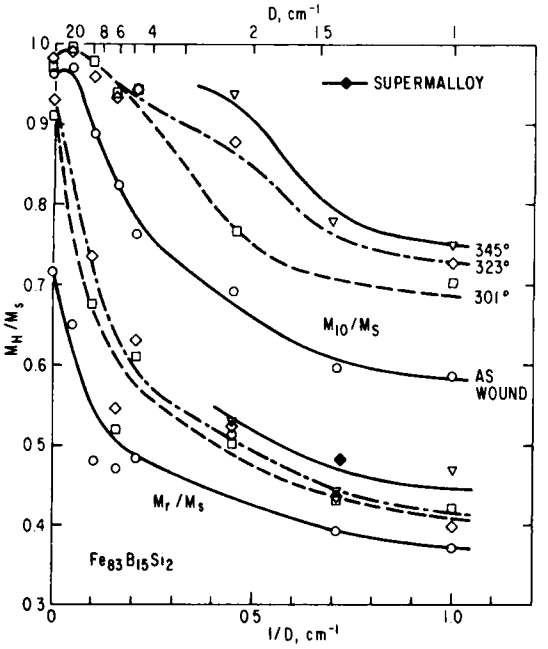

Fig. 2 M_r/M_S and M_{10}/M_S as a function of diameter of the same toroids as in Fig. 1, measured after several thermal treatments for 2 hrs. Note comparison to Supermalloy toroid.

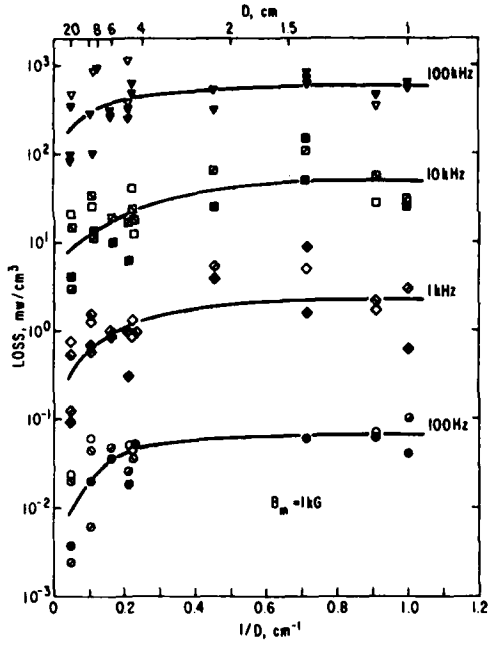

Fig. 3 Loss as a function of toroid diameter measured at various frequencies. ⊗ taken from Luborsky et. al., IEEE Trans. Magnetics, MAG-15 909 (1979) for $Fe_{80}B_{20}$ and $Fe_{82}B_{18}$; ◯, ⊘ $Fe_{82}B_{15}Si_3$ 2.5 mm wide after annealing at 300° and 323°C; ⊘, ● $Fe_{83}B_{15}Si_2$ 1 mm wide after annealing at 300° and 323°C. All annealed in a circumferential field.

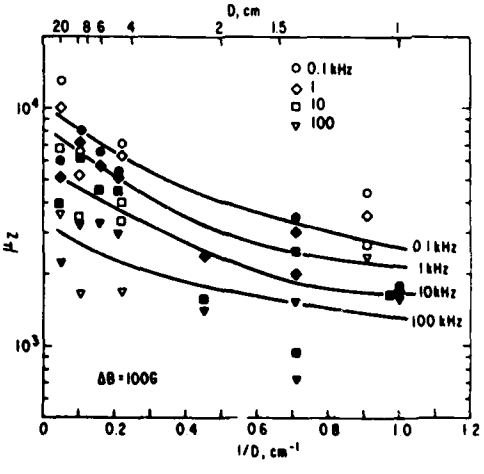

Fig. 4 Impedance permeability as a function of toroid diameter measured at various frequencies for the same samples as in Fig. 3. Open symbols for $Fe_{82}B_{15}Si_3$ obtained by averaging the results of annealing at 300° and 323°C; solid symbols for $Fe_{83}B_{15}Si_2$ obtained by averaging the results of annealing at 300° and 323°C.

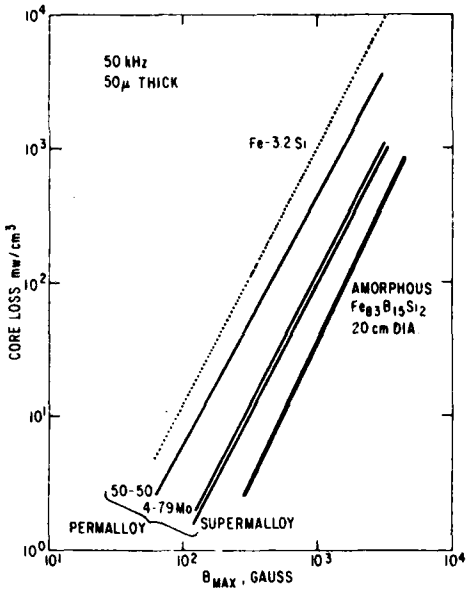

Fig. 5 Core loss at 50 kHz as a function of maximum measuring induction for various commercially available thin tapes compared to our large diameter toroid of amorphous alloy tape.

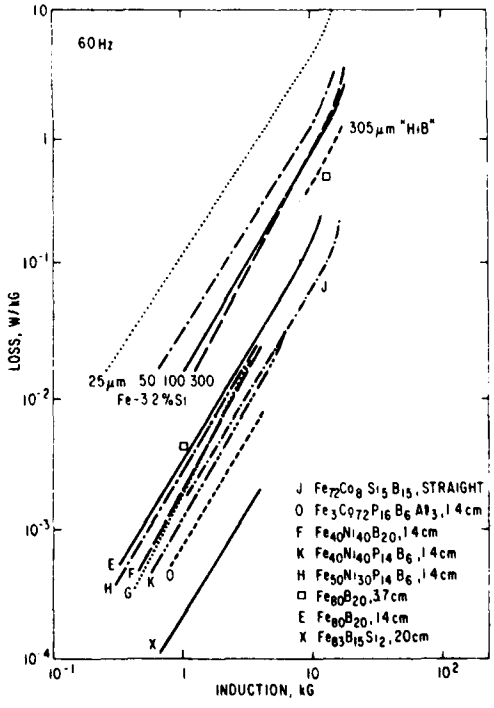

Fig. 6 Core loss at 60 Hz as a function of maximum measuring induction for various amorphous alloys compared to Fe-3.2% Si of various thicknesses. □, O'Handley et. al., J. Appl. Phys. 47, 4660 (1976); X, this work; O, F, K, H, E, Luborsky, Amorphous Magnetism II, edited by R.A. Levy and R. Hasegawa, Plenum Press, 1977, p. 345; J, Fujimori et. al., Rapidly Quenched Metals III, Vol. 2, p. 240 (1978).

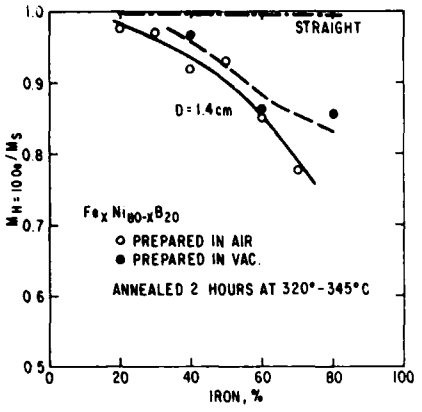

Fig. 7 Magnetization at 10 Oe as a function of iron in $Fe_xNi_{80-x}B_{20}$ amorphous alloys. Straight samples compared to 1.4 cm diameter toroids after stress relief anneal. All ribbons ∿1 mm wide and annealed in a field.

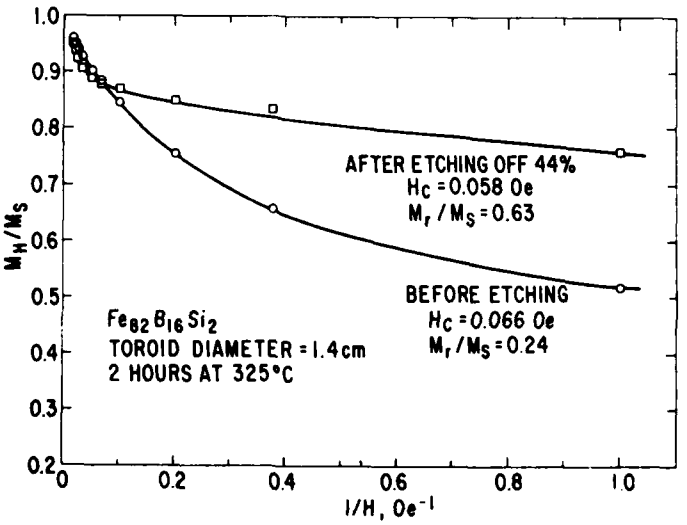

Fig. 8 Magnetization as a function of reciprocal field for a toroid before and after etching off 44% of the inner surface of the 2 mm wide ribbon.

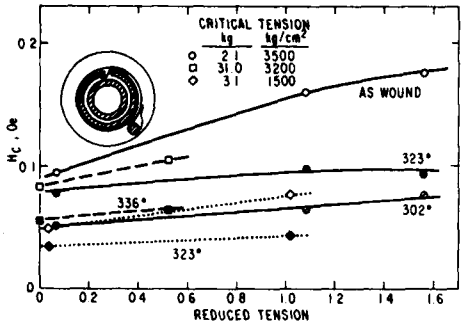

a

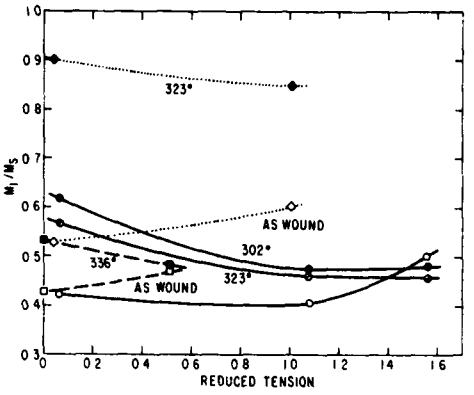

b

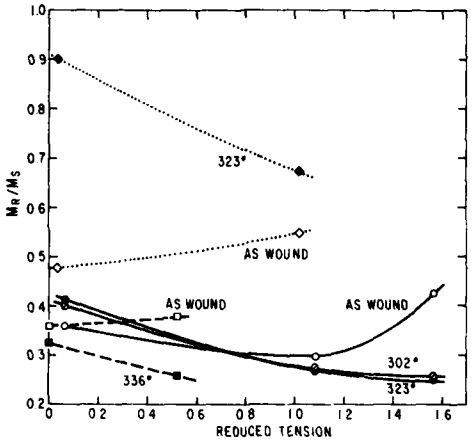

c

Fig. 9 (a) Coercivity of toroids wound under tension. The reduced tension is the ratio of the winding tension to the tension required to reduce the maximum compressive stress to zero. Open symbols as-wound, solid and crossed symbols after 2 hr. anneal in a circumferential field at the temperature indicated. ○ $Fe_{81.7}B_{15}Si_3C_{0.2}Al_{0.1}$, 2 mm wide; □ METGLAS^R 2605B, 2.5 cm wide; ◇ $Fe_{81.5}B_{14.5}Si_4$, 1 cm wide.
(b) Remanence-to-saturation ratio of toroids shown in (a).
(c) Magnetization in 1 Oe field-to-saturation ratio of toroids shown in (a).

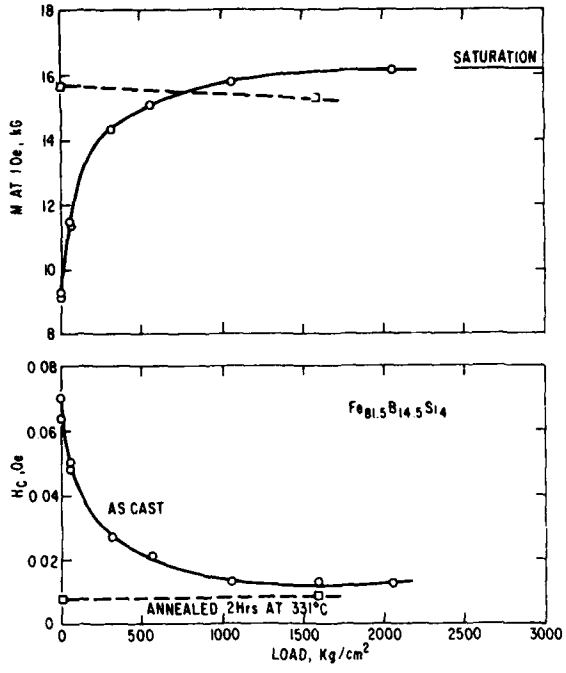

Fig. 10 Effect of applied load on the coercivity and magnetization in 1 Oe field of straight ribbon of $Fe_{81.5}B_{14.5}Si_4$ 1 cm in width. In the case of the annealed sample the load was applied only during the anneal. No field applied during annealing.

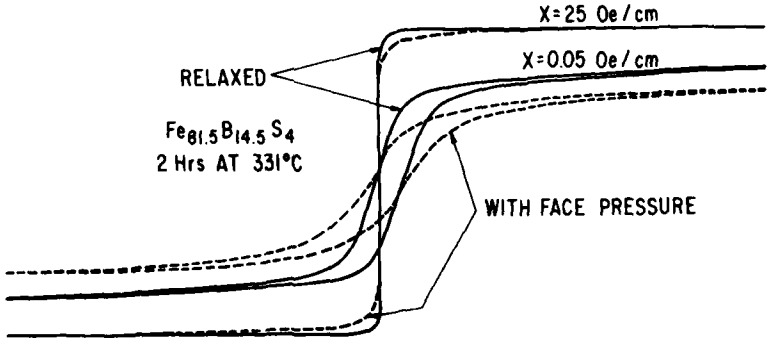

Fig. 11 Hysteresis loops for a relaxed sample 1 cm in width compared to the same sample with compressive tension applied on its face. No field applied during annealing.

GENERAL ELECTRIC

General Electric Company
Corporate Research and Development
Schenectady, New York

TECHNICAL INFORMATION SERIES

AUTHOR
Luborsky, FE Walter, JL
Becker, JJ Martin, DL

NO. 79CRD169
DATE August 1979

TITLE
The Fe-B-C Ternary Amorphous Alloys

GE CLASS 1
NO. PAGES 6

ORIGINATING COMPONENT Metallurgy Laboratory
CORPORATE RESEARCH AND DEVELOPMENT SCHENECTADY, N.Y.

SUMMARY

The properties of amorphous Fe-B-C alloys have been studied. The replacement of boron by carbon reduces the thermal stability of alloys containing more than approximately 80% iron, increases the Curie temperature slightly, and decreases the slope of the magnetization-temperature curve. Thus, although the low-temperature saturation magnetization decreases on replacement of B by C, as expected, the room temperature magnetization exhibits a broad ridge of constant saturation magnetization per gram extending from approximately $Fe_{80}B_{20}$ to approximately $Fe_{83}B_{11}C_6$. This ridge follows one of the low-temperature magnetization contours. The density of the alloys in the series $Fe_{84}B_{16-x}C_x$ was measured and compared to calculated densities. The increase in density agrees with the calculated values and results in a slight increase in saturation magnetization per unit volume with an increase in carbon. The coercivity, both as-cast and after stress relief annealing, increases on replacement of B by C. This is not understood.

SUBJECT
amorphous alloys, magnetic properties

KEY WORDS
amorphous alloys, magnetic properties

INFORMATION PREPARED FOR _____

Additional Hard Copies Available From
Corporate Research & Development Distribution
P.O. Box 43 Bldg. 5, Schenectady, N.Y., 12301

Microfiche Copies Available From
Technical Information Exchange
P.O. Box 43 Bldg. 5, Schenectady, N.Y., 12301

RD-54 (10/70)

THE Fe-B-C TERNARY AMORPHOUS ALLOYS

F.E. Luborsky, J.J. Becker, J.L. Walter and D.L. Martin

INTRODUCTION

This work is part of a study to examine the properties of amorphous alloys and, in particular, alloys containing Fe with different glass-forming metalloids. Ternary Fe-B-C amorphous alloys have recently been reported.[1-6] Hatta et al.[1-4] claim values of $4\pi M_s$ above 16.5 kG, measured at room temperature, for various alloys of $Fe_{100-x-y}B_xC_y$ where the iron content is 84% or higher and the carbon is above about 3-4%. Values of saturation magnetization above 17.5 kG were reported for $Fe_{86}B_7C_7$ after annealing.[3] These values are to be compared to 15.9 to 16.2 kG obtained[7] as the peak value of saturation magnetization in the binary Fe-B amorphous alloys. This peak occurs at $\sim Fe_{80}B_{20}$.[7] However, over the same alloy series of $Fe_{84}B_{16-x}C_x$ and $Fe_{86}B_{14-x}C_x$ studied by Hatta et al., we found no values greater than the saturation magnetization per unit weight for $Fe_{80}B_{20}$ before annealing.[8] It has been found that the replacement of boron by carbon reduces the low temperature moment of the iron and of the alloy.[3] This is expected, based on the simple band theory involving charge transfer since carbon has more electrons available than boron to fill the d-band of the alloy. Thus, Hatta et al. attribute the increase in $4\pi M_s$ at room temperature to:

- An increase in density with addition of carbon.[2]
- A decrease in the slope of the reduced magnetization vs temperature curves at low temperatures.[3]
- A structural change which occurs on annealing.[9]

The decrease in the low-temperature magnetic moment has also been reported by Mitera et al.[5] and by Kazama et al.[6] for alloys of $Fe_{80}B_{20-x}C_x$.

This report describes the formation, magnetic properties, thermal stability, and density of selected amorphous alloys in the ternary Fe-B-C system.

EXPERIMENTAL METHODS

Amorphous ribbons were prepared by melt quenching onto the surface of a rotating wheel.[10,11] Curie temperatures, T_c, were determined using a thermogravimetric recording balance fitted with a permanent magnet to produce a field gradient in a field of 225 Oe. Samples were heated at 20°C/min. Values of saturation magnetization, σ_s, were determined using a vibrating sample magnetometer at fields up to 20 kOe. Results reported were obtained by extrapolating to infinite field using a $1/H^2$ function. Coercive fields, H_c, were determined on 10-cm-long ribbons using an integrating fluxmeter connected to a small sense coil in the center of a long solenoid. Annealing was carried out in a 30-Oe field.

FORMATION

The composition range over which the alloys may be quenched entirely into the amorphous phase is shown in Figure 1. This boundary, of course, will depend on the particular system parameters controlling the quench rate (e.g., melt temperature, ribbon thickness, wheel material, and atmosphere). For the amorphous Fe-B-C alloys prepared in this work, the ribbon thickness was 20-30 μm, the wheel material was copper and casting was done in air. Melt temperatures were not measured. The results reported by Fujimori and Masumoto[12] are essentially the same although no preparation conditions were reported.

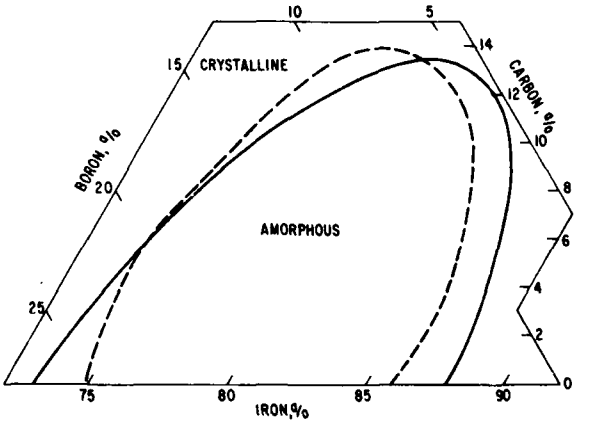

Figure 1. The composition range for the formation of amorphous Fe-B-C alloys. Solid line from this work; dashed line from Fujimori and Masumoto[12]

THERMAL STABILITY

The metallurgical change which occurs when crystallization begins was detected magnetically by two methods. The first method uses the magnetization-temperature curve. The magnetization falls with increasing temperature, typically to M = 0 at T_c. When crystallization starts, iron or compounds with high T_c values appear causing an increase in M. The beginning of this increase in M is denoted as the beginning

Manuscript received June 28, 1979

of crystallization. The M-T curves were taken at the fixed rate of increase of temperature of 20°C/min. The results are shown in Figure 2(a). In the second method we looked for the beginning of the increase in H_c, as measured at room temperature, after successive 2-hour anneals at increasing temperatures. This increase in H_c is associated with the appearance of crystaline phases. The temperature intervals were 25-30°. The results shown in Figure 2(b) do not quite parallel the results in Figure 2(a). Crystallization does start at lower temperatures for the alloys in Figure 2(b), as expected, because of the much slower heating of the incremental step anneals. It is clear that for alloys with greater than approximately 82% Fe, replacement of B by C decreases the stability, or resistance to crystallization. For alloys containing less than approximately 82% Fe the stability first increases and then decreases as B is replaced by C.

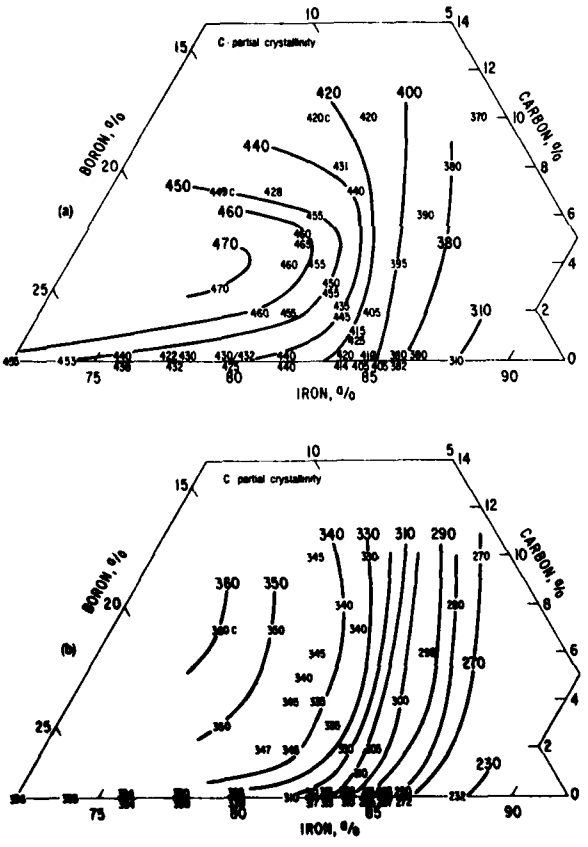

Figure 2. The crystallization temperatures, in °C, for amorphous Fe-B-C alloys obtained at (a) a heating rate of 20°C/min and (b) a 2-hour anneal at increasing temperatures.

It is not clear why this behavior occurs nor why it is different than in the Fe-B-Si amorphous alloys.[13] In the Fe-B-Si alloys the stability increases, over the entire composition range, on replacing B by Si.

MAGNETIC PROPERTIES

Curie Temperature

The Curie temperatures of the Fe-B-C alloys are shown in Figure 3. They show a slight increase in T_c with replacement of B by C for iron contents above about 79%. For iron below about 79%, the T_c decreases slightly on replacement of B by C.

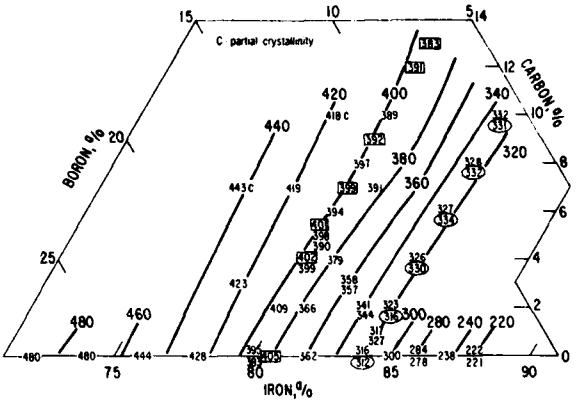

Figure 3. The Curie temperatures, in °C, for amorphous Fe-B-C alloys. Circled results reported by Hatta et al;[1] results in squares from Kazama et al.[6]

Saturation Magnetization

The low-temperature (77 K) saturation magnetization in emu/g, shown in Figure 4(a), exhibits the expected decrease in magnetization with the initial replacement of B by C. This decrease is the result of the greater number of electrons available from the carbon as compared to boron. These additional electrons fill the d-band of the alloy to a greater degree than would be the case for alloys containing only boron, reducing the magnetization. For larger additions of C it appears that σ_s no longer decreases. This is not understandable using the simple charge transfer model. These results have been recalculated in terms of Bohr magnetons per iron atom and are shown in Figure 4(b). In the limit of pure iron, these results approach 2.2, the value for crystalline iron.

The room temperature σ_s values are shown in Figure 5. As in the case for the Fe-B-Si alloys,[13] the σ_s exhibits a ridge of maximum σ_s of constant value out to approximately 6-7% C. The decrease at higher iron contents is caused by the rapid decrease in σ_s as the T_c drops. The ridge, extending out to higher iron contents, is consistent with the shape of the low temperature contours of σ_s. The present results indicate that there is no increase in σ_s with replacement of B by C where Hatta et al.[1-4] observed an increase in σ_s. We have also observed[14] a decrease in the slope of the low temperature reduced magnetization-temperature curve. This will also contribute to the increased room temperature σ_s.

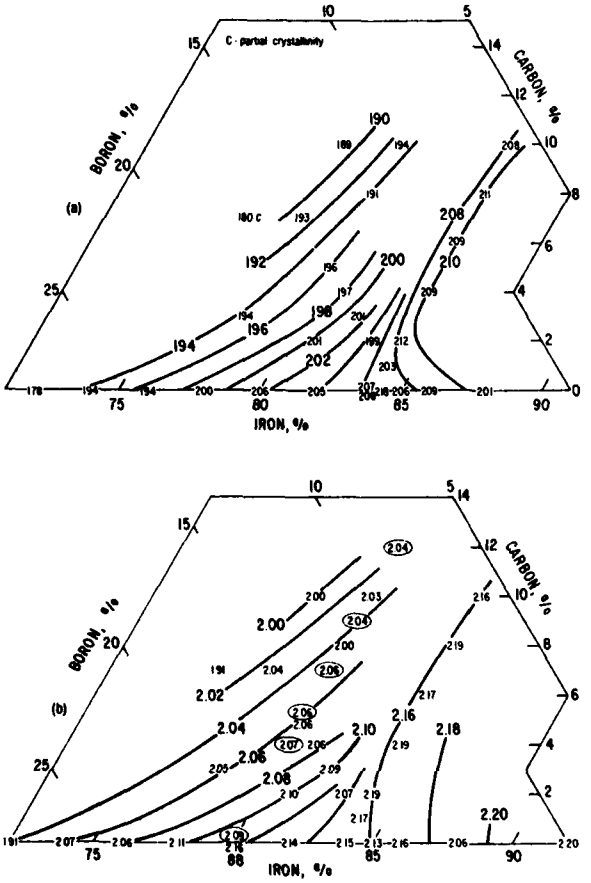

Figure 4. **The saturation magnetization measured at 77 K for amorphous Fe-B-C alloys; (a) in emu/g and (b) in Bohr magnetons per iron atoms, circled results from Kazama et al.[6]**

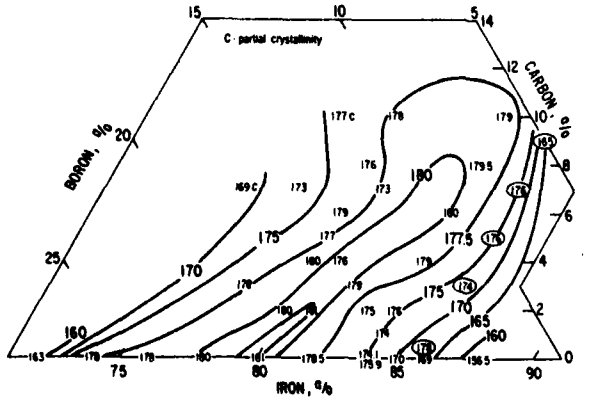

Figure 5. **The saturation magnetization measured at room temperature for amorphous Fe-B-C alloys in emu/g. Circled results from samples prepared by Hatta et al. and measured by us.**

The saturation magnetization has been obtained at 100°C and is shown in Figure 6. This was derived from the magnetization-temperature curve used to determine T_c by normalizing the value at room temperature to the vibrating sample magnetometer measurement at room temperature. As expected, the ridge of maximum σ_s has been moved to lower iron contents and to a lower value since the measurements were made at 100°C; i.e., closer to T_c.

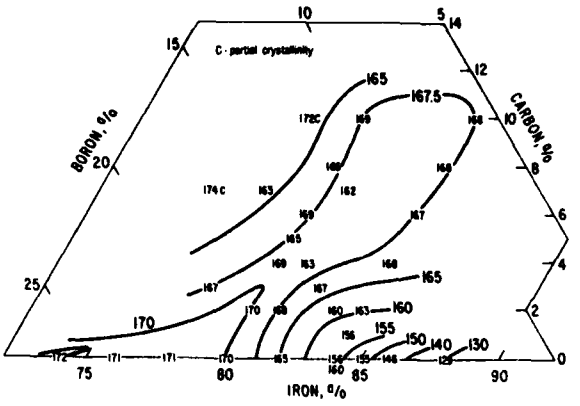

Figure 6. **The saturation magnetization measured at 100°C for amorphous Fe-B-C alloys in emu/g.**

Coercivity

The coercivity of the as-cast Fe-B-C amorphous alloys is shown in Figure 7 and the results after annealing to a minimum in H_c are shown in Figure 8. There appears to be much more scatter in these H_c results than in T_c, σ_s, or stability. This increased scatter is undoubtedly due to the random contributions to H_c from surface irregularities, internal strains, and defects. In any case, the H_c is seen to increase on replacement of B by C both in the as-cast and annealed state. This is the reverse of the behavior in Fe-B-Si alloys on replacement of B by Si.[13]

Density

The results of our density measurements and those of Hasegawa and Ray[16] are compared to calculated values in Figure 9. The curves were derived by first calculating the packing fraction vs iron content of the Fe-B alloy series using the measured densities of Hasegawa and Ray.[16] Then the density of various Fe-B-C alloys was calculated by using these packing fractions for each iron content together with the tetrahedral covalent radii of boron (0.88) and carbon (0.77) as previously described.[17,18]

In this study, the density of a series of $Fe_{84}B_{16-x}C_x$ alloys up to 10 at.% carbon was measured by the buoyancy method by comparing the weight in air to the weight in diethyl phthalate (density of 1.1162 g/cm^3 at 22°C). The density variation of the diethyl phthalate

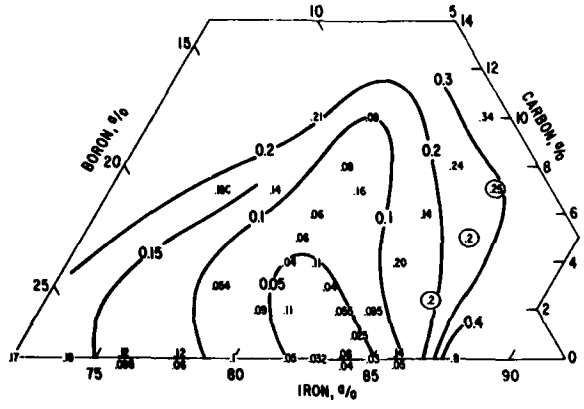

Figure 7. The coercivity, in Oe, for as-cast Fe-B-C amorphous alloys. Circled results from samples prepared by Hatta et al. and measured by us.

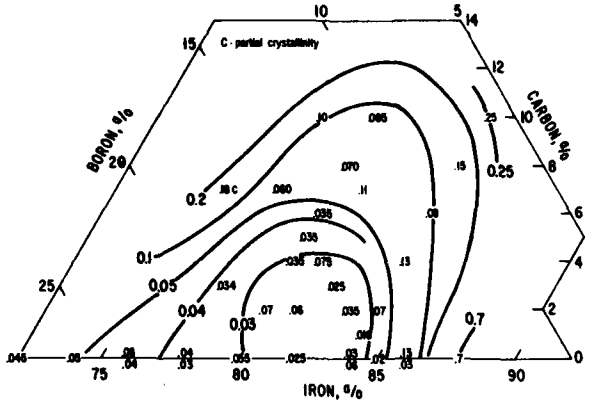

Figure 8. The coercivity, in Oe, for Fe-B-C amorphous alloys annealed to minimum coercivity.

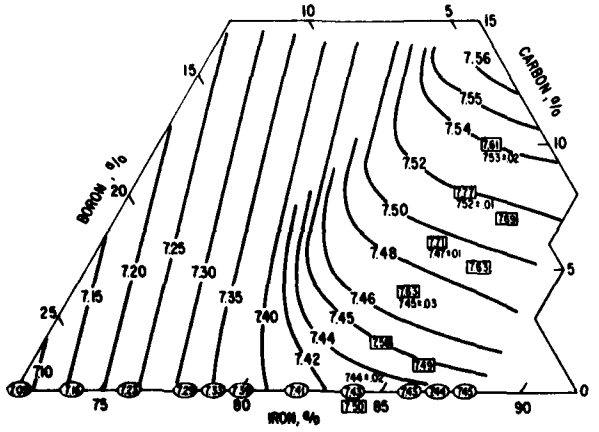

Figure 9. The densities of Fe-B-C amorphous alloys in the as-cast state in g/cm³. Lines calculated as described in the text. The densities with squares around them from Hatta et al.; with circles around them from Hasegawa and Ray; and plain numbers from this work.

with temperature was calculated from that given by $\ln\varrho = -0.000796T + 0.12741$.[15] The samples were cut from ribbons about 1.5 mm wide to give a total sample weight of about 0.22 g. Ten independent density measurements were made on each alloy sample, the results were averaged, and the 99% confidence limit of the mean was determined. Because of the large number of strips needed for each specimen, a special wire holder with a tiny cobalt-samarium magnet fastened to one end was used to hold the strips during weighing in the diethyl phthalate.

Our density measurements for the $Fe_{84}B_{16-x}C_x$ series are given in Figure 9 by the bare numbers and compared in Figure 10 with the calculated values and those reported by Hatta, Egami, and Graham.[2] There is good agreement between our measured density values and the calculated values. Our density values are 1 to 3% lower than those reported by Hatta et al.[2]

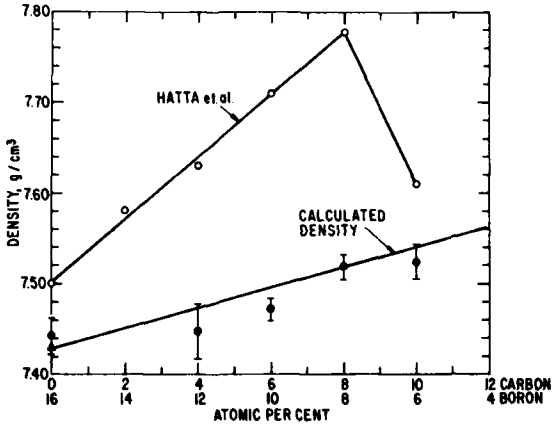

Figure 10. Comparison of our measured density values with the calculated values and those reported by Hatta et al.[2] The error bars represent the 99% confidence interval of the mean.

The $4\pi M_s$ magnetization values of several alloys have been calculated from the density measurements and the saturation magnetization in emu/g from Figure 5. The $4\pi M_s$ value of the $Fe_{80}B_{20}$ alloy was calculated to be 16.8 kG and that for the $Fe_{84}B_{10}C_6$ alloy to be 17.0 kG. As shown by Hatta et al.,[1-4] these values will increase on annealing.

COMPARISON OF Fe-B-C AND Fe-B-Si BEHAVIOR

The region in which the Fe-B-C alloys can be prepared in the amorphous state is qualitatively the same as for the Fe-B-Si alloys although the contour for the transition between the amorphous and crystalline states is tilted to the higher Fe contents for the Fe-B-C alloys. This difference is probably due to differences in the reduced glass temperature, T_g/T_m, where T_m is the melting point. Davies,[19] for example, has shown

that a good correlation exists between the critical cooling rate required for glass formation and T_g/T_m.

The crystallization of Fe-B-C exhibits a decrease in the temperature for the onset of crystallization, T_x, at Fe contents above about 84% as C replaces B but at low Fe contents T_x first increases before decreasing as C replaces B. In the Fe-B-Si alloys, however, the T_x increases as Si replaces B over almost the entire region studied. These differences are probably due to differences in electronic concentrations and in atom sizes.[20]

The changes in the Curie temperature, T_c, with composition are just about the same in the Fe-B-C and Fe-B-Si alloys. This indicates that the near neighbor environment of the Fe atoms is very similar in the two systems. However, Kazama et al.[6] reported that the $Fe_{80}B_{20-x}C_x$ had lower T_c values than $Fe_{80}B_{20-x}Si_x$.

The saturation magnetization at low temperatures shows very similar behavior in the Fe-B-C and Fe-B-Si amorphous alloys. The -Si alloys exhibit slightly higher σ_s as Si replaces B than is observed for C replacing B. This is as expected,[6] since the atomic size of Si is greater than C even though both have the same outer electron configuration and affect the d-band in a similar way.

The saturation magnetization at room temperature is also qualitatively the same in both the Fe-B-C and Fe-B-Si systems as expected from the similarity in T_c and σ_s at low temperature. The difference in behavior of σ_s in the two alloy systems is in the width and length of the ridge of constant maximum σ_s. It is much broader in the Fe-B-C system and extends to lower boron contents than in the Fe-B-Si alloys. This appears to be due to the flatter σ_s vs T curves in the Fe-B-C alloys than in the Fe-B-Si alloys[14] indicating a difference in the long wavelength spin wave spectrum.

Although the behavior of all of the previous properties is qualitatively similar in the Fe-B-C and Fe-B-Si alloys, the behavior of the coercivity is drastically different. In the case of replacement of B by C, H_c increases while on replacement of B by Si, H_c decreases. It is not due to differences in magnetostriction, since measurements[21] on $Fe_{80}B_{20-x}C_x$ and $Fe_{80}B_{20-x}Si_x$ showed no change in magnetostriction for either series of alloys. This behavior is not understood.

CONCLUSIONS

In the ternary Fe-B-C amorphous alloys, the T_c at a constant iron content is almost independent of the boron/carbon ratio. At low temperatures the σ_s decreases on replacement of B by C at constant iron and the moment increases with increase in Fe. However, at room temperature the moment first increases at low Fe contents but then decreases for Fe contents above about 82%. This is due to the decrease in T_c. The coercivity is always higher for the ternary Fe-B-C alloys than for the binary Fe-B alloys. In the region around the ridge of maximum σ_s the crystallization temperature first increases slightly and then decreases as boron is replaced by carbon. Addition of carbon increases the density of the Fe-B alloys by just the amount calculated.

ACKNOWLEDGMENTS

The authors are grateful for the work of N. Marotta in obtaining the Curie temperatures and to J. Gillespie in performing magnetic measurements. The partial support of the Office of Naval Research is also acknowledged.

REFERENCES

1. S. Hatta, T. Egami, and C.D. Graham, Jr., *IEEE Trans. Magn.* MAG-14, 1013 (1978).
2. S. Hatta, T. Egami, and C.D. Graham, Jr., in *Rapidly Quenched Metals III*, Vol. 2, edited by B. Cantor, The Metals Society, London, 1978, p. 183.
3. S. Hatta, T. Egami, and C.D. Graham, Jr., *Appl. Phys. Lett.* 34, 113 (1979).
4. S. Hatta and T. Egami, *J. Appl. Phys.* 50, p. 1589 (March 1979).
5. M. Mitera, M. Naka, T. Masumoto, N. Kazama, and K. Watanabe, *Phys. Status Solidi A* 49, K163 (1978).
6. N.S. Kazama, M. Mitera, and T. Masumoto, in *Rapidly Quenched Metals III*, Vol. 2, edited by B. Cantor, The Metals Society, London, 1978, p. 164.
7. F.E. Luborsky, H.H. Liebermann, J.J. Becker, and J.L. Walter, in *Rapidly Quenched Metals III*, Vol. 2, edited by B. Cantor, The Metals Society, London, 1978, p. 188.
8. F.E. Luborsky, J.J. Becker, and H.H. Liebermann, in *Rapidly Quenched Metals III*, Vol. 2, edited by B. Cantor, The Metals Society, London, 1978, p. 249.
9. T. Egami, *J. Appl. Phys.* 50, p. 1564 (March 1979).
10. H.H. Liebermann and C.D. Graham, Jr., *IEEE Trans. Magn.* MAG-12, 921 (1976).
11. J.L. Walter, in *Rapidly Quenched Metals III*, Vol. 1, edited by B. Cantor, The Metals Society, London, 1978, p. 30.
12. H. Fujimori and T. Masumoto, *Suppl. to Sci. Rep. Res. Inst., Tohoku Univ.*, Ser. A 27, 181 (1978).
13. F.E. Luborsky, J.J. Becker, J.L. Walter, and H.H. Liebermann, *IEEE Trans. Magn.* MAG-15, p. 1146 (1979).
14. F.E. Luborksy, J.J. Becker, J.L. Walter, and H.H. Liebermann, *J. Magn. Magn. Mater.*, to appear.
15. H.C. Rogers, R.C. Leech and L.F. Coffin, Final Report, Contract NOw-65-0097-f, Naval Air Systems Command (Nov. 1965).
16. R. Hasegawa and R.Ray *J. Appl. Phys.* 49, 4174 (1978).
17. G.S. Cargill III, *Solid State Phys.* 30, 227 (1975).

18. F.E. Luborsky, *Ferromagnetic Materials,* edited by E.P. Wohlfarth, North Holland Publ. Co., Amsterdam, 1979, to appear.
19. H.A. Davies, *Phys. Chem. Glasses*, 17, 159 (1976).
20. I.W. Donald and H.A. Davies, in *Rapidly Quenched Metals III*, Vol. 1, edited by B. Cantor, The Metals Society, London, 1978, p. 273.
21. F.E. Luborsky, P.J. Flanders, H.H. Liebermann, and J.L. Walter, *IEEE Trans. Magn.*, to appear.

GENERAL ELECTRIC

General Electric Company
Corporate Research and Development
Schenectady, New York

TECHNICAL INFORMATION SERIES

AUTHOR: Luborsky, FE Frischmann, PG Johnson, LA	SUBJECT: Amorphous alloys	NO.: 79CRD209 DATE: December 1979
TITLE: Amorphous Materials — A New Class of Soft Magnetic Alloys		GE CLASS: 1 NO. PAGES: 6
ORIGINATING COMPONENT: Metallurgy Laboratory		CORPORATE RESEARCH AND DEVELOPMENT SCHENECTADY, N.Y.

SUMMARY

The key events in the development of amorphous alloys are briefly summarized within the context of applying them as soft magnetic alloys. This report reviews some of their pertinent magnetic properties, such as saturation magnetization, losses, exciting current, permeability, and stress sensitivity and compares them to conventional alloys. Additionally, the report presents new results on iron-rich alloys. We have recently discovered that increasing the diameter of the toroid prepared from narrow tapes produces a remarkable *improvement* in the magnetic properties attributable to the decreasing contribution of stress-induced ordering. The losses become significantly less than the best results reported for the Permalloys and are much less than one tenth the losses of Fe-3.2% Si.

KEY WORDS

amorphous alloys, soft magnetic materials

INFORMATION PREPARED FOR _____

Additional Hard Copies Available From

Corporate Research & Development Distribution
P.O. Box 43 Bldg. 5, Schenectady, N.Y., 12301

Microfiche Copies Available From

Technical Information Exchange
P.O. Box 43 Bldg. 5, Schenectady, N.Y., 12301

RD-54 (10/70)

AMORPHOUS MATERIALS—A NEW CLASS OF SOFT MAGNETIC ALLOYS

F.E. Luborsky, P.G. Frischmann, and L.A. Johnson

INTRODUCTION

In the first papers[1,2] on the potential application of amorphous alloys as soft magnetic materials, attention focused mainly on static magnetic properties such as coercivity, H_c; remanence, B_r; saturation magnetization, $4\pi M_s$; Curie temperature, T_c; and the effect of annealing and stress on these properties. Later papers[3-9] discussed losses and permeabilities in the general context of potential applications. Various devices were studied and their requirements reviewed.[5-9] This paper briefly reviews the material properties important to various classes of devices and then discusses recent results aimed at developing the understanding of the relation between these device-oriented parameters and fundamental parameters.

MATERIAL PROPERTIES COMPARISONS

In electronic-type applications, where varius nickel-iron alloys are presently used, available amorphous alloys have lower losses, higher B_r and $4\pi M_s$, and equivalent or lower H_c values. However, amorphous alloys tend to have lower T_c, lower magnetic stability, lower initial permeabilities, and higher stress sensitivities.

In power devices such as large distribution transformers, which presently use Fe-3¼% Si, the amorphous alloys have considerably lower losses, lower H_c, and higher permeabilities. However, the $4\pi M_s$ is approximately 15% lower than Fe-Si. This is considered a major drawback adding to the final transformer's overall cost.

SATURATION MAGNETIZATION

In recent years there has been considerable exploration[10-20] into methods of raising $4\pi M_s$ of low cost amorphous alloys. Of necessity this exploration has attempted to modify the basic Fe-B amorphous alloy by replacing some of the B with other metalloids and by annealing. Additions of Co or Ni are considered too costly. Some[14] have claimed that replacement of boron with carbon to make $Fe_{86}B_7C_7$ raises $4\pi M_s$ from 16.1 kG for the $Fe_{81}B_{19}$ (the peak value in the Fe-B alloys), to 17.4 kG. Approximately two hours of annealing at 270 °C further raises this to 17.8 kG. However, these reported values depend on the density used, and the densities Hatta et al.[14] reported are about 3% higher than the densities Luborsky et al.[17] reported. Figure 1[17] shows the ternary corner of the Fe-B-C diagram for

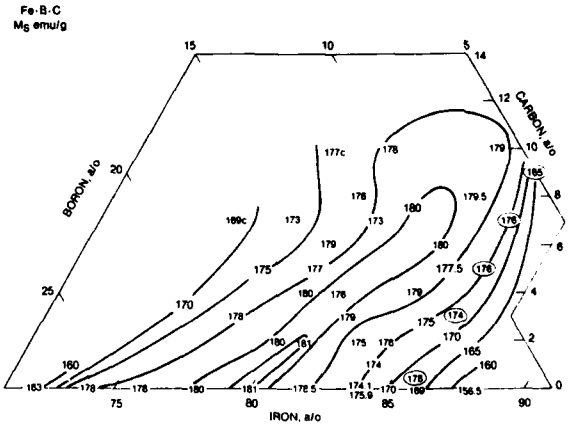

Figure 1. Saturation magnetizations in emu/g at room temperature in the ternary Fe-B-C amorphous alloys.

iso-magnetization curves measured at room temperature in emu/g. By measuring the $4\pi M_s$ in emu/g one avoids the problem of measuring the density in order to convert to Gauss. These curves show that a ridge of constant $4\pi M_s$ in emu/g extends out from $Fe_{80}B_{20}$ to $Fe_{83}B_9C_8$. Since the density increases about 1.8% from 7.38_5 to 7.51_5 g/cm^3,[17] this means that $4\pi M_s$ in Gauss measured at room temperature also increases about 1.8%, or from 16.1 to 16.4 kG. As Figure 2 shows,[15] similar iso-magnetization curves have also been generated for the Fe-B-Si alloys. In this case the ridge of constant $4\pi M_s$ is much narrower than for the Fe-B-C alloys, and it extends from $Fe_{80}B_{20}$ to only $Fe_{82}B_{12}Si_6$. The densities for the Fe-B-Si alloys have not been reported before. They are calculated here, as previously described,[17] and compared to a few measured values, as Figure 3 shows. The agreement between calculated and measured values, as observed also for the Fe-B-C alloys, is excellent. Thus the density decreases in going from $Fe_{80}B_{20}$ to $Fe_{83}B_{12}Si_6$, i.e., from 16.1 to 16.0 kG. More recently we have examined the properties of Fe-B-Si-C alloys and found the T_c, M_s, and H_c behavior to be a more or less additive function of the individual Fe-B-Si and Fe-B-C parameters. However, the ease of preparation and the resultant stability of the quaternary alloys appear better than for either of the constituent tenary alloys.

Manuscript received August 30, 1979

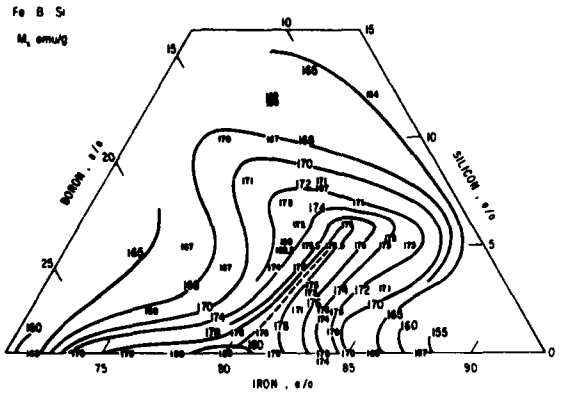

Figure 2. Saturation magnetizations in emu/g at room temperature in the ternary Fe-B-Si amorphous alloys.

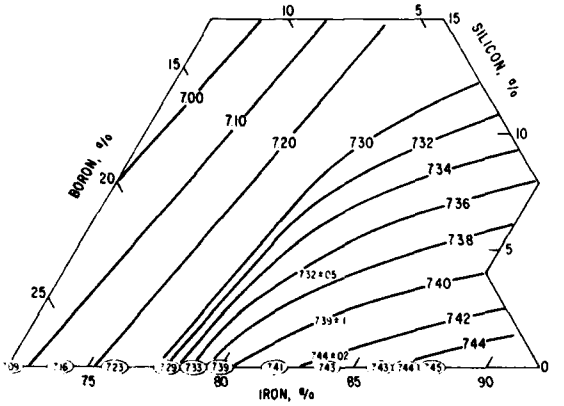

Figure 3. Density in g/cm³ at room temperature in the ternary Fe-B-Si amorphous alloys. Curves calculated. Circled numbers from R. Hasegawa and R. Ray, *J. Appl. Phys.* 49 (1978) 4174. Small numbers measured by D. L. Martin, unpublished.

Preliminary results on Fe-B-Ge ternary amorphous alloys indicate that replacement of B by Ge indeed raises T_c considerably, as previously reported,[21,22] and that σ_s at room temperature has a similar ridge of constant value. However, the density increases 4% from 7.38$_5$ to 7.7 g/cm³, corresponding to an increase in room temperature $4\pi M_s$ from 16.1 to 16.7 kG before annealing, compared to 16.4 kG in the Fe-B-C system.

One must also consider the effect of elevated temperatures since most transformers operate at temperatures as high as 100 °C. In the case of Fe-Si, the $4\pi M_s$ value is virtually the same at 25 °C and 100 °C because Fe-Si's T_c is so high (~755 °C). However, the amorphous alloys with their relatively low T_c (~370 °C) are found to have a reduction of $4\pi M_s$ equal to 6% for $Fe_{81.5}B_{13.5}C_5$ and 7% for $Fe_{81.5}B_{13.5}Si_5$. In the case of Fe-B-Ge alloys, T_c increases substantially and thus the effect of temperature should be smaller.

LOSSES

As a result of studies on the effect of strain-induced anisotropy[23] (caused by the winding stresses introduced in toroids), a major improvement in losses was recently reported.[25] It was found, for example, that in narrow amorphous alloy tapes the properties improved remarkably as the diameter of the toroid increased. Thus a 20-cm diameter toroid had roughly 1/10 the losses of a 1.4-cm diameter toroid. At 60 Hz these losses represent the lowest losses of any alloy reported so far. Figure 4 compares these losses to those of all other amorphous alloys reported so far, from zero magnetostrictive alloys, given by the dotted curve labeled O, to the high magnetization alloys labeled E, all measured on small diameter toroids. Other reported alloys[3] have losses which fall between O and E, as the crosshatched area indicates. The curve labeled L indicates the losses of the commercially available Fe-B-Si-C amorphous alloy (METGLAS® 2605SC). For comparison, Figure 4 also shows results on various grades of Fe-3.2% Si alloys. The thin tapes, 25 to 100 μm thick, are used in small electronic devices and have poor losses because of the poor orientation developed in these thicknesses. The 280 to 355 μm thick Fe-Si have good orientation and, up until the past few years, were used exclusively in high quality distribution and power transformers and other specialized devices. The newer Hi-B variety, originally

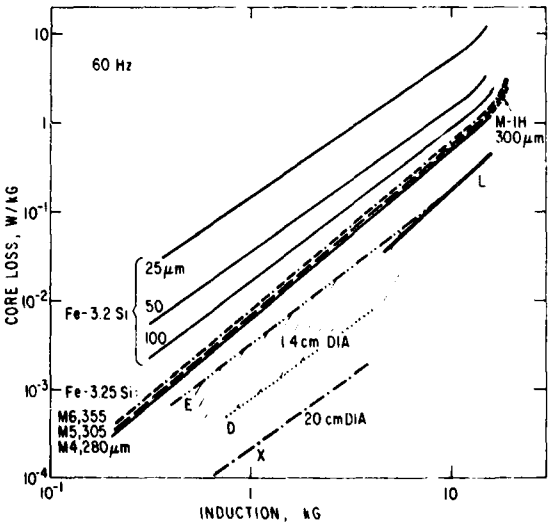

Figure 4. Core losses vs. induction for Fe-3¼% Si alloys and for amorphous alloys, all measured at 60 Hz. The 25-, 50-, and 100-μm Fe-Si tapes from *Arnold Bulletin 5C-107A*, March 1963. M4, M5, M6 Fe-Si sheet from *Armco Catalog*, 1974. M-1H Fe-Si from *Nippon Steel Cat. EXE 320*, 1976. E = $Fe_{80}B_{20}$ 1.4-cm diam. narrow tape;[3] crosshatched area enclosed all other curves for amorphous alloys;[3] X = $Fe_{81}B_{13}Si_2$ 20-cm diam. narrow tape;[23] L = $Fe_{81.5}B_{13.5}Si_{3.5}C_2$ METGLAS® 2605SC from *Allied Chem. Co. Bulletin* 6/79.

developed in Japan,[24] achieves even lower losses with improved grain orientation, improved tension effect of the coating, reduced sheet thickness and grain size, and reduction of inclusions and internal stresses. These Hi-B alloys are now used in modern high quality distribution and power transformers.

The new results on losses of the 20-cm diameter toroid are now less than those reported for any of the best commercial Ni-Fe alloys. Figure 5 compares at 50 kHz these results to previous results on high magnetization $Fe_{80}B_{20}$ and to commercially available Fe-B-Si-C (METGLAS® 2605SC). This improvement in losses for the 20-cm diameter toroid holds at all frequencies. Thus, as far as losses are concerned, the amorphous alloys are clearly better than any of the best commercial alloys. Furthermore, they have the considerably higher $4\pi M_s$ of 16 kG, compared to 8 kG for 4-79 Mo Permalloy and Supermalloy, and the same 16 kG as the 50-50 Permalloy but they are lower than the 20 kG of the Fe-3.2% Si.

PERMEABILITY

Figure 6 shows the permeabilities at $\Delta B = 100$ G, i.e., near the initial permeability range for some commercial Fe-Si and Ni-Fe alloys and for some amorphous alloys. The crosshatched area corresponds to the range of results previously reported[3] for amorphous alloys from zero magnetostriction with the highest μ_z, to high magnetization $Fe_{80}B_{20}$ alloys with lower μ_z. In addition, Figure 6 shows the new results on the 20-cm diameter toroid and some results from Allied Chemical Company data sheets for their Fe-B-Si-C alloy (METGLAS® 2605SC). Except for zero magnetostrictive alloys,[25] the permeability at 60 Hz of 30,000 for METGLAS® 2826MB is probably among the highest yet reported for amorphous alloys.[25] However, these values are still considerably below the 4-79 Mo-Permalloy and the Supermalloy. It is not clear why higher values of μ_z have not yet been achieved.

Figure 7 shows results similar to those in Figure 6 but for permeabilities near their maximum value. A similar sequence is shown but with the amorphous

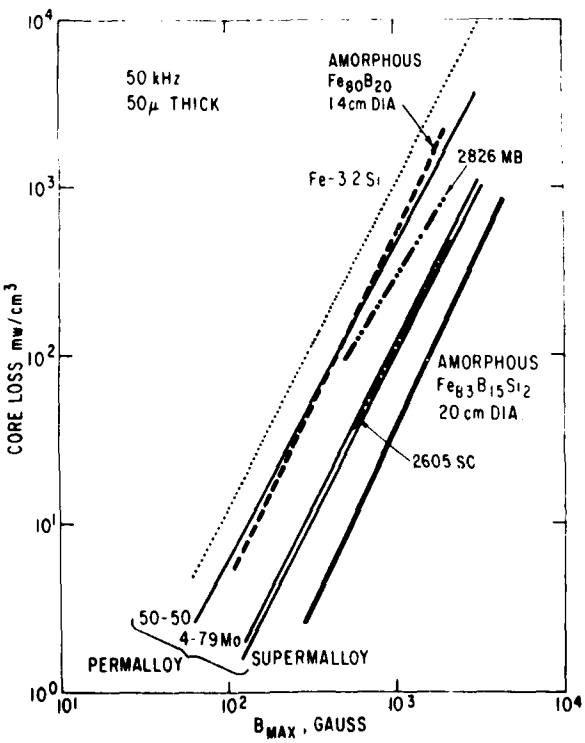

Figure 5. **Core losses vs. induction measured at 50 kHz for 50-μm-thick Permalloys and 30-μm-thick amorphous $Fe_{83}B_{15}Si_2$ of narrow ribbon measured as a 20-cm diameter toroid.[23] $Fe_{80}B_{20}$ from (3), METGLAS® 2605SC and 2826 MB from *Allied Chem. Co. Bulletin* 6/79.**

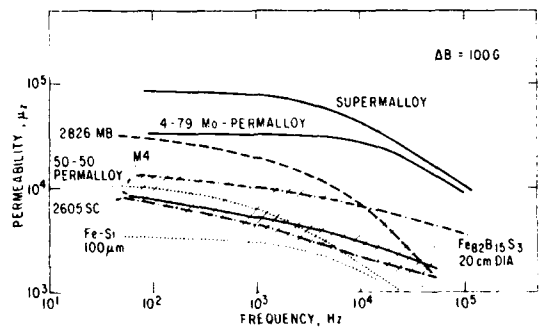

Figure 6. **Impedance permeability measured at $\Delta B = 100$ G vs. frequency for various Permalloys from *Arnold Cat. TC-101B*, 1972; Fe-3¼% Si grade M4 305-μm thick from *Armco Cat.* 1974; METGLAS® 2605SC and 2826MB amorphous alloys from *Allied Chem. Co. Bulletin* 6/79; and $Fe_{82}B_{15}Si_3$ amorphous alloy 20-cm diam. toroid from narrow tape.[23]**

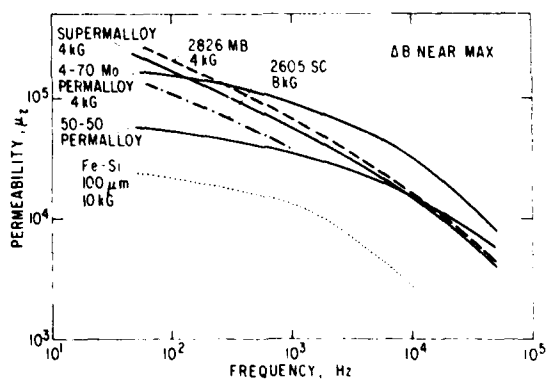

Figure 7. **Impedance permeability measured near its peak value as a function of frequency for various Permalloys and FeSi thin tape from *Magnetic Metals Cat. C1-171-20M* and for METGLAS® alloys from *Allied Chem. Co. Bulletin* 6/79.**

alloys reaching higher values of μ_z (max) than the corresponding Permalloy, i.e. METGLAS® 2826MB should be compared to Supermalloy and 4-79Mo-Permalloy of similar $4\pi M_s$ and METGLAS® 2605SC should be compared to 50-50 Permalloy, of similar $4\pi M_s$. It is believed that the more rapid fall off with frequency for the amorphous alloys compared to the Permalloys is the result of their rougher surface. Values of μ(max) for dc fields of greater than 2×10^6 have been reported for various $(Fe_{1-x}Ni_x)$-Si-B alloys.[26] This is well above any of the values expected from Figure 7 at low frequencies.

EXCITATION POWER

Very little has been reported on the very important parameter in amorphous alloys of excitation power for evaluating distribution transformer performance. This was first reported in 1978[6] for small 1.4-cm diameter toroids of $Fe_{80}B_{20}$ and $Fe_{40}Ni_{40}P_{14}B_6$. New results in Figure 8 are from our own measurements and from Allied Chemical Company compared to results on Fe-Si. The amorphous alloys are clearly superior to 50 μm Fe-Si tapes.

We can compare the amorphous alloys to Hi-B or M-4 Fe-Si in different ways. First, the induction developed at the same exciting power occurs at 1 VA/kG and gives B = 13.5 kG. Second, for amorphous alloys the knee occurs at ~0.45 VA/kG compared to ~1.5 VA/kG, i.e., a factor of three smaller, but B ≃12.5 kG compared to 17 kG, i.e., ≃25% lower than the Fe-Si. We may also compare the ratio of the value of B at the knee to the value of B at saturation. For amorphous alloys this ratio is 12.6/16.1 = 0.78 while the value for Fe-Si is 17.0/20 = 0.85. Thus, we expect some further improvements in the amorphous alloys.

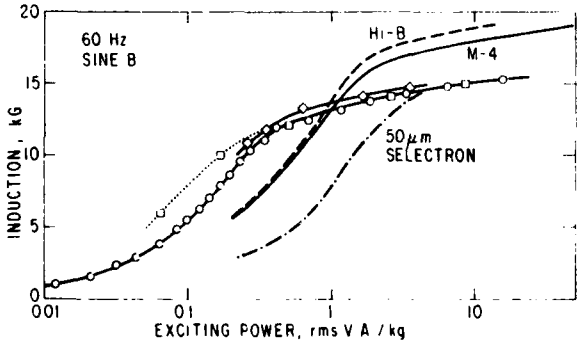

Figure 8. Induction vs. exciting power measured at 60 Hz for varius Fe-3¼% Si alloys, M4 280-μm thick from *Armco Cat.* 1974; Hi-B 300-μm thick from Nippon Steel Corp. Cat. EXE 320, 1975; Selectron from *Arnold Bulletin SC-107A* 1963; □ METGLAS® 2605SC amorphous alloys from *Allied Chem. Co. Bulletin* 6/79; METGLAS® 2605SC amorphous alloy toroid prepared in this work with 13.9 cm o.d. 7.9 cm i.d. and 2.5 cm height unbonded; the same core after impregnation bonding.

STRESS SENSITIVITY

In the oriented Fe-Si alloys any anisotropy caused by stress must compete with the rather large crystal anisotropy of 3.5×10^5 ergs/cm^3. In the iron-rich, stress-relieved amorphous alloys the only anisotropy present is probably field-induced and may be in the order of 1×10^3 ergs/cm^3.[27] Thus, even for alloys with the same magnetostriction (and the oriented Fe-Si and amorphous Fe-B-Si have similar magnetostrictions), the effect of a given stress will be much larger on the amorphous alloy. Furthermore, the application of a coating which imparts a stress to the Fe-Si reduces the effective magnetostriction. Such coatings have not yet been developed for the amorphous alloys.

There have been various reports[1,23] on the effect of tensile stresses on the properties of amorphous alloys. These tensile stresses interact with the positive magnetostriction to decrease H_c and increase B_H/B_s. On winding a toroid it is desirable to wind with high tension in order to increase the packing fraction. It was first thought that this high tension in the toroid would indeed enhance the properties as observed on applying tension to straight ribbons. However, just the reverse was observed,[23] as indicated by the increase in H_c on winding toroids shown in Figure 9. A similar decrease in B_H/B_s was also reported. This deterioration was demonstrated[23] to be the result of simultaneous application of face pressure which develops as tension is applied during toroid winding. We now report, in Figure 10, on the effect of applying only face pressure to the amorphous alloy. Face pressure was developed by applying a static load on the face of a stack of about 75 rings chemically etched out of 2.5-cm wide tape. The load was applied between three segments of windings onto a thick glass ring to distribute the load evenly. The windings

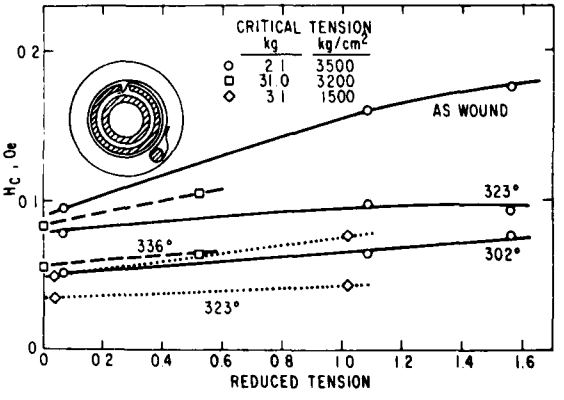

Figure 9. Coercivity of toroids wound under tension. The reduced tension is the ratio of the winding tension to the critical tension required to reduce the maximum compressive stress to zero. Open symbols, as-wound; solid and crossed symbols after 2 hr. anneal in a circumferential field at the temperature indicated. $Fe_{82}B_{15}Si_3$, 2 mm wide; □ METGLAS® 2605B, 2.5 cm wide; $Fe_{81.5}B_{14.5}Si_4$, 1 cm wide.

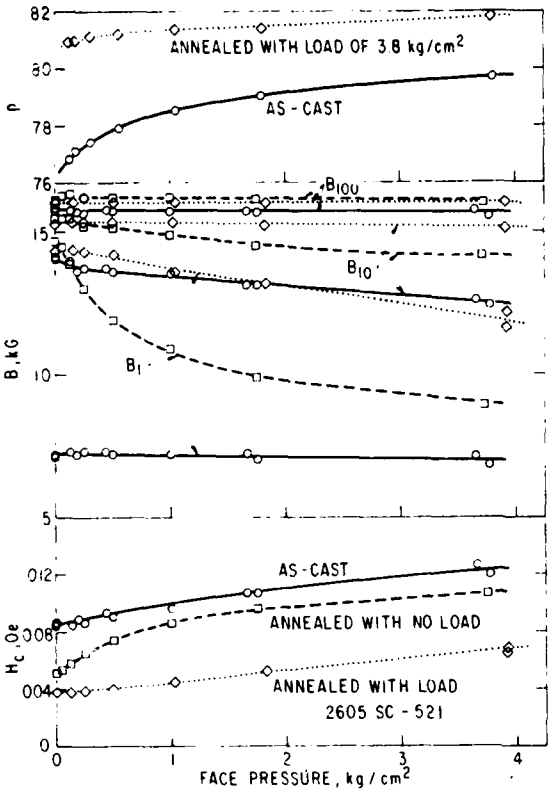

Figure 10. The effect of face pressure on magnetic properties and packing fraction of rings before and after annealing of METGLAS® 2605SC.

were connected to a standard hysteresigraph. The face stress sensitivity of the as-cast rings, both in B and H_c, is much less than after annealing in a field with a 4 kG/cm^2 load, and both of these show much less stress sensitivity than the rings annealed in a field with no load. This is the expected sequence since the as-cast samples have the highest anisotropy and the samples annealed with no load have the lowest anisotropy. The application of face pressure will produce a random planar contribution to the easy axis which in the case of the annealed specimen, for example, does not change the easy axis-planar anisotropy although there will be a change in the out-of-plane anisotropy. Thus, there should be no change in the magnetization curve. This view, of course, ignores the possible effects of frictional constraints on the ideal expansion of the compressed ring samples which could contribute to a compressive stress component along the ribbon length. This could contribute to the observed behavior. Furthermore, surface irregularities will not only enhance stress enhancement, but will also yield stress components in various unwanted directions.

Using the same fixture, the packing fraction was measured as a function of face pressure by noting the compression of the stack of rings. Figure 10 also shows these results. The large dependence of packing on pressure for the as-cast rings is expected because the random variations in flatness which the rings exhibited. Annealing with a load, of course, flattened and compressed the stack, resulting in higher packing and less dependence of packing on pressure.

SUMMARY AND CONCLUSIONS

In the past year or two the saturation magnetization has been increased from 16 to approximately 17 kG by substituting carbon for some boron. Further improvements may occur by substituting with germanium. Losses have also improved substantially, now achieving levels well below the best Permalloys, but the permeabilities reported have only increased slightly. More attention must now be paid to the exciting power required to reach various induction values. Finally, one must consider the extreme stress sensitivity of the amorphous alloys in fabricating and using these alloys.

ACKNOWLEDGMENTS

The authors wish to thank the Office of Naval Research for their support.

REFERENCES

1. T. Egami, P.J. Flanders, and C.D. Graham, Jr., *AIP Conf. Proc.* No. 24 (1975) 697.
2. E.M. Gyorgy, H.J. Leamy, R.C. Sherwood, and H.S. Chen, *AIP Conf. Proc.* No. 29 (1976) 198.
3. F.E. Luborsky, in *Amorphous Magnetism II*, R.A. Levy and R. Hasegawa, ed. (Plenum Press, NY 1977) p. 345.
4. F.E. Luborsky, P.G. Frischmann, and L.A. Johnson, *J. Magnetism Magn. Mat. 8* (1978) 318.
5. F.E. Luborsky, J.J. Becker, P.G. Frischmann, and L.A. Johnson, *J. Appl. Phys. 49* (1978) 1769.
6. F.E. Luborsky, *IEEE Trans. Magnetics MAG-14* (1978) 1008.
7. K.J. Overshott, *Electronics and Power Mag.* (1979) 347.
8. R. Hasegawa and R.C. O'Handley, *J. Appl. Phys. 50* (1979) 1551.
9. W. Wolf, R. Mohn, and U. Konig, *J. Magnetism Magn. Mat. XX* (1980).
10. K. Hoselitz, in *Rapidly Quenched Metals III*, B. Cantor, ed. (The Metals Soc., London, 1978) Vol. 2, p. 245.
11. S. Hatta, T. Egami, and C.D. Graham, Jr., in *Rapidly Quenched Metals III*, B. Cantor, ed., (The Metals Soc., London, 1978) Vol. 2, p. 183.
12. F.E. Luborsky, J.J. Becker, and H.H. Liebermann, in *Rapidly Quenched Metals III*, B. Cantor, ed. (The Metals Soc., London, 1978) Vol. 2, p. 249.
13. S. Hatta, T. Egami, and C.D. Graham, Jr., *IEEE Trans. Magnetics MAG-14* (1978) 1013.
14. S. Hatta, T. Egami, and C.D. Graham, Jr., *Appl. Phys. Lett. 34* (1979) 113.

15. F.E. Luborsky, J.J. Becker, J.L. Walter, and H.H. Liebermann, *IEEE Trans. Magnetics MAG-15* (1979) 1146.
16. R.C. O'Handley, C.-P. Chou, and N. DeCristofaro, *J. Appl. Phys.*, to appear.
17. F.E. Luborsky, J.J. Becker, J.L. Walter, and D.L. Martin, *IEEE Trans. Magnetics MAG-15* (1979).
18. M. Mitera, T. Masumoto, and N.S. Kazama, to appear.
19. K. Hoselitz, *Phys. Stat. Sol.* [*a*] *53* (1979) K23.
20. K. Hoselitz, *J. Magnetism Mag. Mat.*, to appear.
21. M. Mitera, M. Naka, T. Masumoto, N. Kazama, and K. Watanabe, *Phys. Stat. Sol.* [*a*] *49* (1978) K163.
22. N.S. Kazama, M. Mitera, and T. Masumoto, in *Rapidly Quenched Metals III*, B. Cantor, ed., (The Metals Soc., London, 1978) Vol. 2, p. 164.
23. F.E. Luborsky and J.J. Becker, *IEEE Trans. Magnetics MAG-15* (1979).
24. S. Taguchi, *Trans. I.S.I.J. 17* (1977) 604.
25. S. Ohnuma and T. Masumoto, in *Rapidly Quenched Metals III*, B. Cantor, ed., (The Metals Soc., London, 1978) Vol. 2, p. 197.
26. T. Masumoto, K. Watanabe, M. Mitera, and S. Ohnuma, in *Amorphous Magnetism II*, R.A. Levy and R. Hasegawa, ed., (Plenum Press, NY 1977) p. 369.
27. F.E. Luborsky and J.L. Walter, *IEEE Trans. Magnetics MAG-13* (1977) 953.

BASIC DISTRIBUTION LIST SRD-80-006

Technical and Summary Reports January 1980

Organization	Copies
Defense Documentation Center Cameron Station Alexandria, VA 22314	12
Office of Naval Research Department of the Navy 800 N. Quincy Street Arlington, VA 22217	
ATTN: Code 471	1
Code 102	1
Code 470	1
Commanding Officer Office of Naval Research Branch Office Building 114, Section D 666 Summer Street Boston, MA 02210	1
Commanding Officer Office of Naval Research Branch Office 536 South Clark Street Chicago, IL 60605	1
Office of Naval Research One Hallidie Plaza Suite 601 San Francisco, CA 94102	1
Naval Research Laboratory Washington, DC 20375	
ATTN: Codes 6000	1
6100	1
6300	1
6400	1
2627	1
Naval Air Development Center Code 302 Warminster, PA 18964 ATTN: F.S. Williams	1
Commander MERADCOM DRDME-EA Fort Belvoir, VA 22060 ATTN: J.H. Ferrick	1

Organization	Copies
Naval Air Propulsion Test Center Trenton, NJ 08628 ATTN: Library	1
Naval Construction Batallion Civil Engineering Laboratory Port Hueneme, CA 93043 ATTN: Materials Division	1
Naval Electronics Laboratory San Diego, CA 92152 ATTN: Electron Materials Sciences Division	1
Naval Missile Center Materials Consultant Code 3312 -1 Point Mugu, CA 92041	1
Commanding Officer Naval Surface Weapons Center White Oak Laboratory Silver Spring, MD 20910 ATTN: Library	1
David W. Taylor Naval Ship Research and Development Center Materials Department Annapolis, MD 21402	1
Naval Undersea Center San Diego, CA 92132 ATTN: Library	1
Naval Underwater System Center Newport, RI 02840 ATTN: Library	1
Naval Weapons Center China Lake, CA 93555 ATTN: Library	1
Naval Postgraduate School Monterey, CA 93940 ATTN: Mechanical Engineering Department	1

DISTRIBUTION LIST (Cont'd)

Organization	Copies
Naval Air Systems Command Washington, DC 20360	
ATTN: Codes 52031	1
52032	1
Naval Sea System Command Washington, DC 20362 ATTN: Code 035	1
Naval Facilities Engineering Command Alexandria, VA 22331 ATTN: Code 03	1
Scientific Advisor Commandant of the Marine Corps Washington, DC 20380 ATTN: Code AX	1
Naval Ship Engineering Center Department of the Navy Washington, DC 20360 ATTN: Code 6101	1
Army Research Office P.O. Box 12211 Triangle Park, NC 27709 ATTN: Metallurgy and Ceramics Program	1
Army Materials and Mechanics Research Center Watertown, MA 02172 ATTN: Research Programs Office	1
Air Force Office of Scientific Research Bldg. 410 Bolling Air Force Base Washington, DC 20332 ATTN: Chemical Science Directorate Electronics & Solid State Sciences Directorate	1
Air Force Materials Laboratory Wright-Patterson AFB Dayton, OH 45433	1
Library Building 50, Rm 134 Lawrence Radiation Laboratory Berkely, CA	1

Organization	Copies
NASA Headquarters Washington, DC 20546 ATTN: Code RRM	1
NASA Lewis Research Center 21000 Brookpark Road Cleveland, OH 44135 ATTN: Library	1
National Bureau of Standards Washington, DC 20234 ATTN: Metallurgy Division	1
Inorganic Materials Div.	1
Director Applied Physics Laboratory University of Washington 1013 Northeast Fortieth Street Seattle, WA 98105	1
Defense Metals and Ceramics Information Center Battelle Memorial Institute 505 King Avenue Columbus, OH 43201	1
Metals and Ceramics Division Oak Ridge National Laboratory P.O. Box X Oak Ridge, TN 37380	1
Los Alamos Scientific Laboratory P.O. Box 1663 Los Alamos, NM 87544 ATTN: Report Librarian	1
Argonne National Laboratory Metallurgy Division P.O. Box 229 Lemont, IL 60439	1
Brookhaven National Laboratory Technical Information Division Upton, Long Island New York 11973 ATTN: Research Library	1
Office of Naval Research Branch Office 1030 East Green Street Pasadena, CA 91106	1

DISTRIBUTION LIST (Cont'd)

Name	Copies
Professor G.S. Ansell Rensselaer Polytechnic Institute Department of Metallurgical Engineering Troy, NY 12181	1
Professor Dieter G. Ast Cornell University Department of Materials Science and Engineering Ithaca, NY 14853	1
Dr. E.M. Breinan United Technologies Corporation United Technologies Research Center East Hartford, CT 06108	1
Professor H.D. Brody University of Pittsburgh School of Engineering Pittsburgh, PA 14213	1
Dr. R.W. Cahn University of Sussex School of Engineering and Applied Science Brighton BN1 9QT ENGLAND	1
Dr. E.A. Clark Solid State Division Naval Surface Weapons Center White Oak Laboratory Silver Spring, MD 20910	1
Dr. S.M. Copley University of Southern California Los Angeles, CA 90007	1
Professor M. Cohen Massachusetts Institute of Technology Department of Metallurgy Cambridge, MA 02139	1
Dr. B. Diegle Battelle 505 King Avenue Columbus, OH	1
Professor B.C. Giessen Northeastern University Department of Chemistry Boston, MA 02115	1
Professor N.J. Grant Massachusetts Institute of Technology Department of Materials Science and Engineering Cambridge, MA 02100	1
Dr. J. Perel Phrasor Technology 1536 Highland Avenue Duarte, CA 91010	1
Professor O.D. Sherby Stanford University Materials Science Division Stanford, CA 94300	1
Professor D. Turnbull Harvard University Division of Engineering and Applied Physics Cambridge, MA 02138	1
Professor R. Mehrabian University of Illinois Department of Mechanical and Industrial Engineering Urbana, IL 61801	1
Professor P.R. Strutt University of Connecticut School of Engineering Department of Metallurgy Storrs, CT 06268	1